Thermochimica Acta 503–504 (2010) 70–84

Contents lists available at ScienceDirect

Thermochimica Acta

journal homepage: www.elsevier.com/locate/tca

# Crosslink density dependence of polymer degradation kinetics: Photocrosslinked acrylates

Vadim V. Krongauz*

*Baxter Healthcare Corporation, Device Center of Excellence, Applied Science and Technology, Materials Dpt., Rt. 120 & Wilson Rd., RLT-14, Round Lake, IL 60073, USA*

ARTICLE INFO

*Article history:*
Received 20 January 2010
Received in revised form 8 March 2010
Accepted 11 March 2010
Available online 19 March 2010

*Keywords:*
Polyacrylate
Thermal
Degradation
Kinetics
Crosslink density
Thermogravimetry-mass spectrometry

ABSTRACT

A series of crosslinked polyurethane acrylate films with glass transition temperatures ranging from −49 °C to +65 °C was prepared by photopolymerization of solvent-free resins. The kinetics of thermo-oxidative (in air) and thermal (in $N_2$) degradation of these crosslinked acrylate networks at temperatures from 100 °C to 400 °C was monitored thermogravimetricly as a function of crosslink density. Initial degradation rate of polyurethane network decreased with the increase of crosslink density. Apparent activation energies of degradation were found to be temperature and crsosslink density dependent and ranged from 12.6 kJ mol$^{-1}$ to 25.1 kJ mol$^{-1}$ in 200–300 °C interval and 33.5 kJ mol$^{-1}$ to 58.6 kJ mol$^{-1}$ in 300–400 °C interval. The polyacrylate thermal stability increase with crosslinking was correlated with decreased chain segments mobility leading to the reduced oxygen and volatile products diffusion rate, rate of cyclic decarboxylation, and increased radical's recombination in a cage. Data indicated that the cyclic decarboxylation, rather than oxygen uptake or volatile products escape rate control the thermal degradation kinetics.



## 1. Introduction

Polymer degradation mechanism was and is extensively studied (Schemes 1–5) [1,2, ref. therein, 3–6]. There is however a disparity in the published data on crosslinking effects on polymer degradation rate [7–13]. It was stated that crosslinking (and polymer crystallization) inhibited thermo-oxidation due to slower oxygen diffusion into polymer [1,8], however it was also reported that lower chain mobility *decreased* thermal stability of the polymer [9]. No change was observed in epoxy networks aging resistance with increased crosslinking [10]. Thermal aging induced stress-relaxation time increase was reported to become larger with crosslink density increase [1,11]. Stability increase with degree of crosslinking was reported for vulcanized cis-1,4-polyisoprene [12,13]. The changes of stability were attributed to decrease in the rate of oxygen diffusion into highly crosslinked systems, without reference to degradation in the oxygen-free environment [1–7,9,14]. It was also reported that thermal degradation kinetics was affected by a crosslinking method [15,16]. The structure of crosslinking bridging bonds also influenced crosslinking effect on degradation of polymers. Thus, sulfur vulcanized polyisoprene rubber was less stable than peroxide vulcanized rubber [12]. The rate of degradation was found to be proportional to the chain length between the crosslinks [13]. "To further complicate the problem of gaining comparative stability data, an enormous body of literature has been compiled from "off-the-shelf" polymers and routine thermal analysis data on materials of unknown structure" [7, p. 4].

Formal and statistical approaches to kinetics of polymer degradation were developed [1,2,4,7,14,17,18], and higher stability of crosslinked polymers was also attributed to the lower probability of bond scission due to thermal fluctuations [19]. To the best of my knowledge, Transition State Theory approach [20–22] was not applied to polymer degradation kinetics, thus change in vibrational energy distribution in highly crosslinked systems was not considered.

Derivation of mechanism of degradation based on thermogravimetric measurements alone was questioned in the past, since only the volatile products loss was monitored [23]. However, thermogravimetry allows direct and sensitive monitoring of relative changes in degradation kinetics of different polymers. Mass-spectrometry adds monitoring and identification of specific volatile products of polymer degradation. Non-volatile insoluble degradation remnants can be analyzed by infrared spectroscopy. When polymer thermal degradation mechanism is established, TG-Mass-spectral and infrared spectroscopy based kinetic data can be successfully interpreted [1,2,7,24–45].

Thermal stability dependence on crosslink density was revisited in the current work. It was postulated in the past that volatiles loss rate controlled the observed degradation kinetics of large samples [37,38]. Degradation was monitored gravimetrically, and by a combination of thermogravimetry

* Tel.: +1 847 270 4270; fax: +1 847 270 4490.
*E-mail address:* vadim_krongauz@baxter.com.

0040-6031/$ – see front matter © 2010 Elsevier B.V. All rights reserved.
doi:10.1016/j.tca.2010.03.011

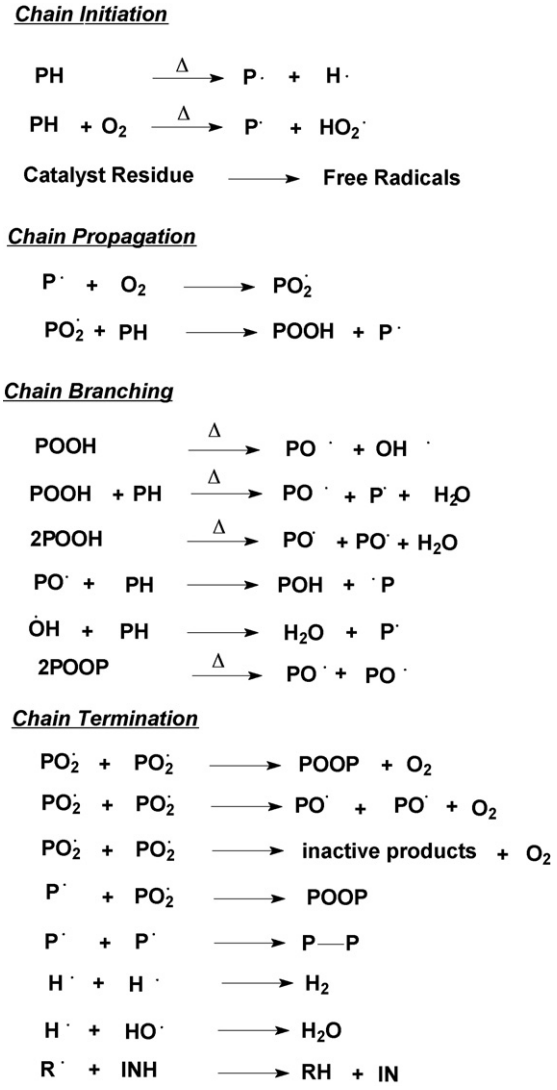


**Scheme 1.** Kinetic model of thermo-oxidative degradation of polymers [1,2,7,24].

with mass-spectrometry. Mass-spectral differential monitoring of volatiles loss rate was used in the present work to verify this postulated assertion. To eliminate the uncertainties of "of-the-shelf polymer" analysis [7–16] a series of aliphatic urethane acrylate resins was formulated by us to produce, upon photo-curing, polymeric films of known composition with well-defined glass transition temperatures ($T_g$) and crosslink density (deduced using dynamic mechanical analysis). The choice of radiation curable acrylates was stipulated by high reproducibility of produced polymers, absence of additives, good film formation; most importantly, the chemical mechanism of thermal and thermo-oxidative degradation of polyacrylates was established in the past (Schemes 2–5) [1,2,7,24–45].

Polyacrylates degradation in air occurs through peroxides formation, radical reactions with oxygen with depolymerization, formation of alcohols, carbon dioxide, etc. (Schemes 1–3) [1,2]. In the absence of oxygen, polyacrylates degrade through re-arrangements leading to decarboxylation, and formation of monomer and alcohols (Schemes 4 and 5) [7,24–45]. In the presence of oxygen, formation of alcohol, decarboxylation and depolymerization take place by different reaction paths and the polymer degradation rate is usually higher (Schemes 2 and 3) [7,24,46–48]. Polymers with higher crosslink density are expected to be more stable due to reduced mobility of radicals (higher cage recombination probability), slower oxygen ingress and volatile products evaporation, slower "valency transfer" [1,3–6]. Crosslink density controls chain segments mobility and according to Eyring relative rates of

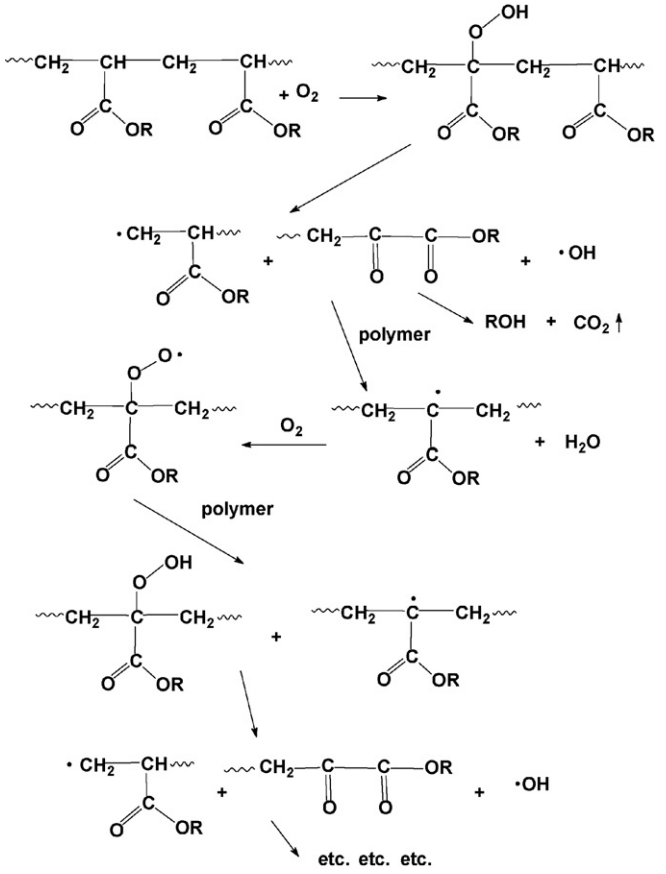


**Scheme 2.** Likely route of volatile products formation upon thermo-oxidative degradation of polyacrylates [7,24,46–48].

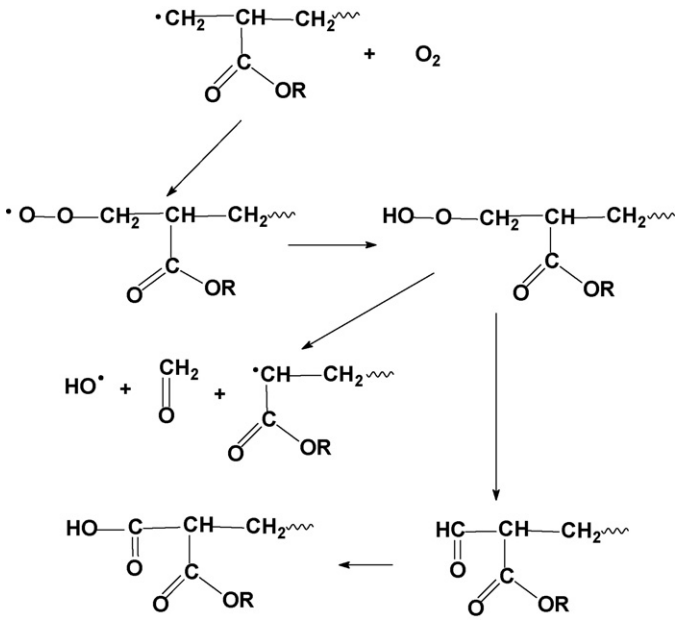


**Scheme 3.** Path for aldehydes and acids formation during thermo-oxidative degradation of polyacrylates [7,24,46–48].

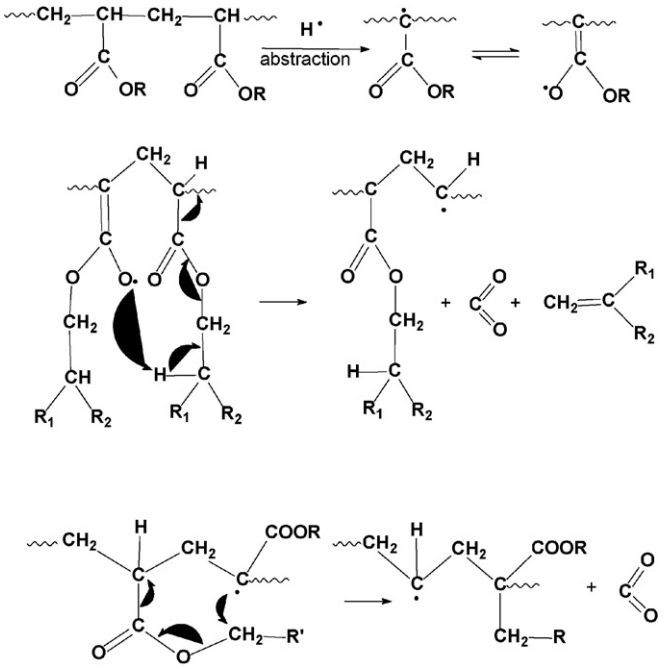


**Scheme 4.** Likely mechanism of acrylates decarboxylation in the absence of oxygen [7,24–45].

oxygen diffusion and volatile products escape, potentially altering degradation kinetics [49–52]. We compared kinetics of degradation with and without oxygen to understand degradation rate- controlling process in highly crosslinked polymers.

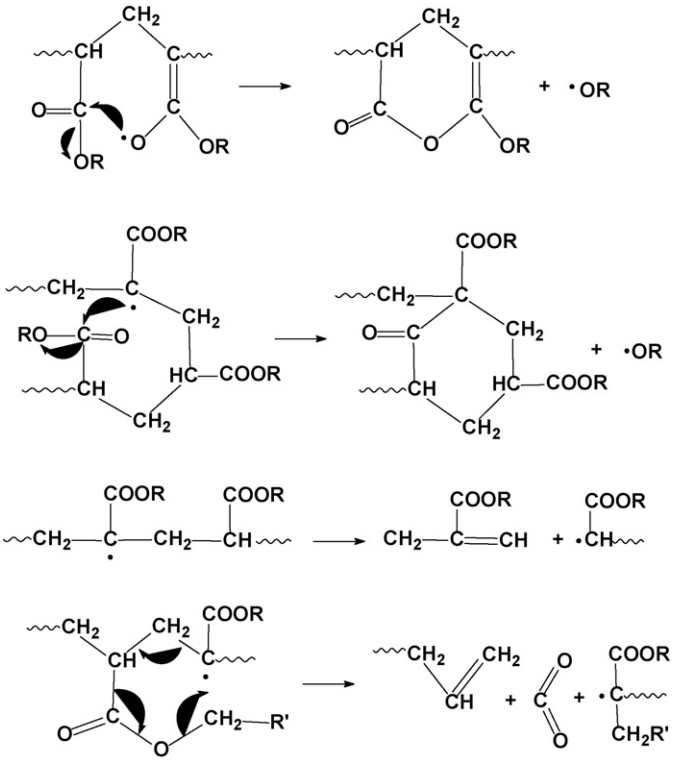


**Scheme 5.** Additional possible routes for volatile products formation upon oxygen-free thermal degradation of polyacrylates [7,24–45].

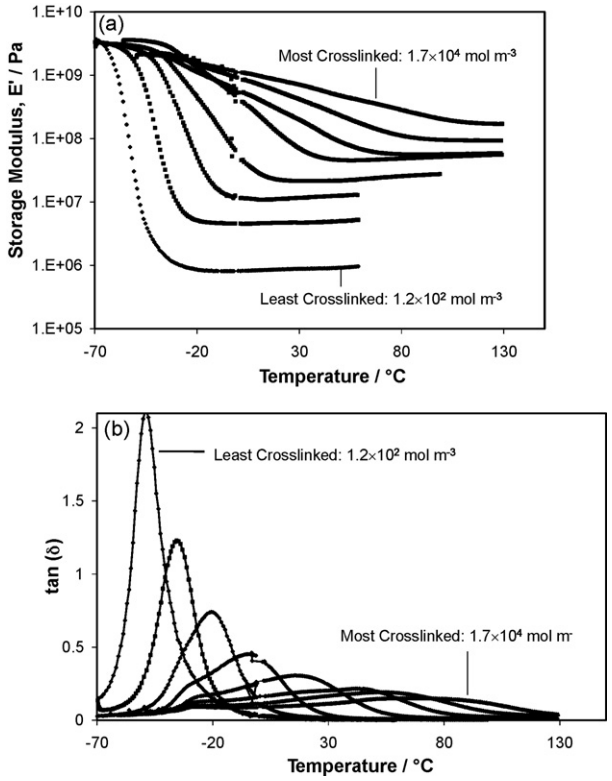


**Fig. 1.** Results of dynamic mechanical analysis of the UV-cured crosslinked polyurethane acrylate films. The highest crosslink density was $1.7 \times 10^4$ mol m$^{-3}$, while the lowest was $1.2 \times 10^2$ mol m$^{-3}$ (Table 2).

## 2. Experimental

### 2.1. Instrumentation and processes

The resins were cured using a microwave discharge lamp at 0.5 mJ cm$^{-2}$ (Conveyor belt system, Fusion UV Systems Inc.). UV dose was monitored prior to cure with Profiling Belt Radiometer, ILT 400, UVA (International Light Technology). The completeness of polymerization (>90% acrylate double bond conversion) was verified by acrylate double bond infrared absorption at 810 cm$^{-1}$ (Nicolet 8700 FTIR Spectrometer Mainframe with Smart Orbit accessory and diamond crystal plate, Thermo Electron North America LLC).

Dynamic mechanical analysis (DMA) (RSA3, TA Instruments) was conducted in a tensile mode at 1.0 Hz, using 5–6 mm wide, 100–200 μm thick film strips. The data were processed to yield glass transition temperatures and crosslink densities of the polyurethane acrylates, according to common practices based on a position of maximum of loss tangent, tan $\delta$ (Fig. 1) [5,6,53–55].

TGA was conducted in isothermal and temperature rump modes in oxygen or in dry nitrogen flow of 60 cm$^3$ min$^{-1}$ using TGA 2950 system (TA Instruments). TGA-Mass-spectrometry was conducted using TGA Q500 (TA Instruments) interfaced (200 °C heated interface) with ThermoStar$^{TM}$ mass spectrometer (Pfeiffer Vacuum Inc.). TGA-mass-spec monitoring was conducted in $N_2$ flow of 60 cm$^3$ min$^{-1}$. The film sample, ≈5 μg, was placed in an opened platinum pan. Isothermal conditions were achieved through equilibrating the sample at 30 °C for 10 min, raising the temperature to a desired value (100 °C, 200 °C, 300 °C, or 400 °C), then maintaining this temperature for 90 min (Fig. 2). Temperature ramp experiments were conducted at 10 °C/min temperature increase rate from 30 °C to 450 °C (Fig. 2). In all of the air-free experiments nitrogen was allowed to flow through the cell for 10 min after closing the

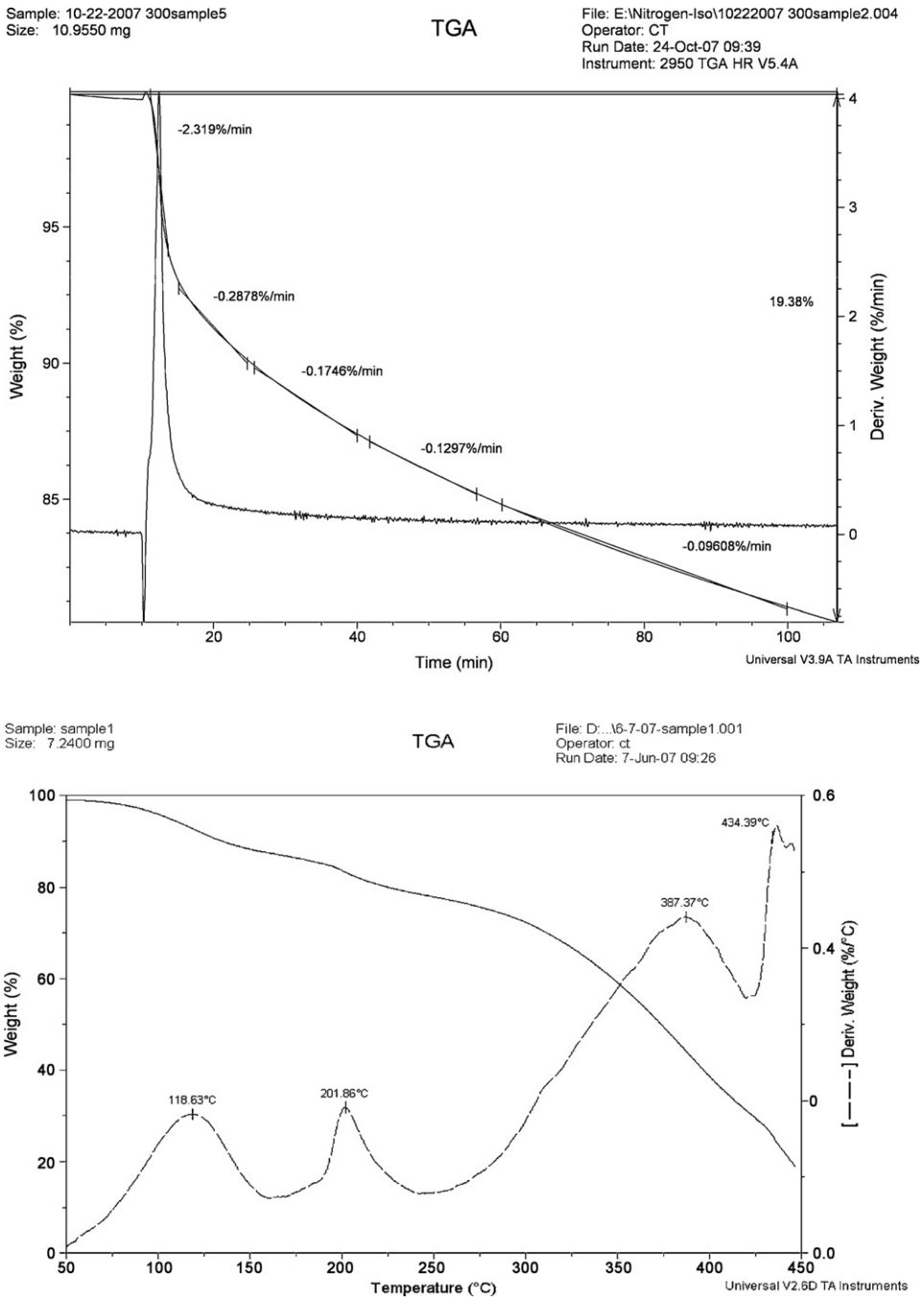


**Fig. 2.** Gravimetrically detected kinetics of thermal degradation of crosslinked polyurethane acrylate.

cell and prior to the beginning of the heating cycle. Attenuated Total Reflection (ATR) spectra of the non-volatile remains were obtained using Nicolet 8700 FTIR Spectrometer Mainframe with Smart Orbit accessory and diamond crystal plate (Thermo Electron North America LLC) (Fig. 3).

### 2.2. Materials

Oligomers and monomers were purchased from Sartomer Co., and initiators were from Ciba Specialty Chemicals Co. (Table 1). Commonly synthesized and commercially available oligomers are polyols or polyesters end-capped with acrylate either through ester, or through urethane bridge [56–60]. Number of urethane groups is usually twice the number of acrylate groups in oligomer [59]. Difunctional urethane acrylate oligomer, CN966B85, was selected since it yielded more flexible polymer solids [56–61]. The variation of glass transition temperature was accomplished by varying difunctional monomer concentration [59,60]. The concentration of difunctional urethane acrylate oligomer was constant to reduce variability in degradation rates due to the urethane functional group presence.

## 3. Results and discussion

Glass transition temperatures of cured polyacrylates varied from −49 °C to +65 °C (Fig. 1 and Table 2). No loss of volatiles was observed below 200 °C. Thermal degradation of urethane and ester bridges above 200 °C was accompanied by depolymerization and

**Table 1**
Composition of resins forming photocrosslinked acrylate networks.[a].

| Sample No. | Initiator[a] Irgacure 651 (%) | Initiator[a] Irgacure 184 (%) | Oligomer[a] difunctional CN966B85 (%) | Monomer[a] SR256 (%) | Monomer[a] difunctional SR238 (%) | Total difunctional acrylates (monomer + oligomer)[b] (%) |
|---|---|---|---|---|---|---|
| 1 | 3 | 2 | 25 | 70 | 0 | 3.75 |
| 2 | 3 | 2 | 25 | 60 | 10 | 13.75 |
| 3 | 3 | 2 | 25 | 50 | 20 | 23.75 |
| 4 | 3 | 2 | 25 | 40 | 30 | 33.75 |
| 5 | 3 | 2 | 25 | 30 | 40 | 43.75 |
| 6 | 3 | 2 | 25 | 20 | 50 | 53.75 |
| 7 | 3 | 2 | 25 | 10 | 60 | 63.75 |
| 8 | 3 | 2 | 25 | 0 | 70 | 73.75 |

[a] Irgacure 651(Ciba): α,α,-dimethoxy-α-phenylacetophenone; Irgacure 184 (Ciba): 1-hydroxy-cyclohexyl-phenyl-ketone; SR256 (Sartomer): 2(2-ethoxyethoxy)ethyl acrylate; SR238 (Sartomer): 1,6-hexanediol diacrylate; CN966B85 (Sartomer): urethane acrylate oligomer/monomer blend.
[b] CN966B85 contains 15% SR238.

**Table 2**
Glass transition temperatures derived from dynamic mechanical analysis (DMA) data of the UV-cured acrylic films.

| Sample No. | Total difunctional acrylates (crosslinking) (%) | $T_g$ (°C) | Rubbery plateau tensile storage modulus, $E'$ (MPa) | Crosslink density, $\nu_e$ (mol m$^{-3}$) |
|---|---|---|---|---|
| 1 | 3.75 | −48.7 | 0.96 | $1.2 \times 10^2$ |
| 2 | 13.75 | −35.6 | 5. 21 | $6.3 \times 10^2$ |
| 3 | 23.75 | −20.6 | 12.96 | $15.7 \times 10^2$ |
| 4 | 33.75 | −4.8 | 27.47 | $29.7 \times 10^2$ |
| 5 | 43.75 | 16.4 | 55.79 | $55.8 \times 10^2$ |
| 6 | 53.75 | 43.5 | 58.72 | $58.8 \times 10^2$ |
| 7 | 63.75 | 52.9 | 93.32 | $93.3 \times 10^2$ |
| 8 | 73.75 | 65.2 | 170.00 | $169.7 \times 10^2$ |

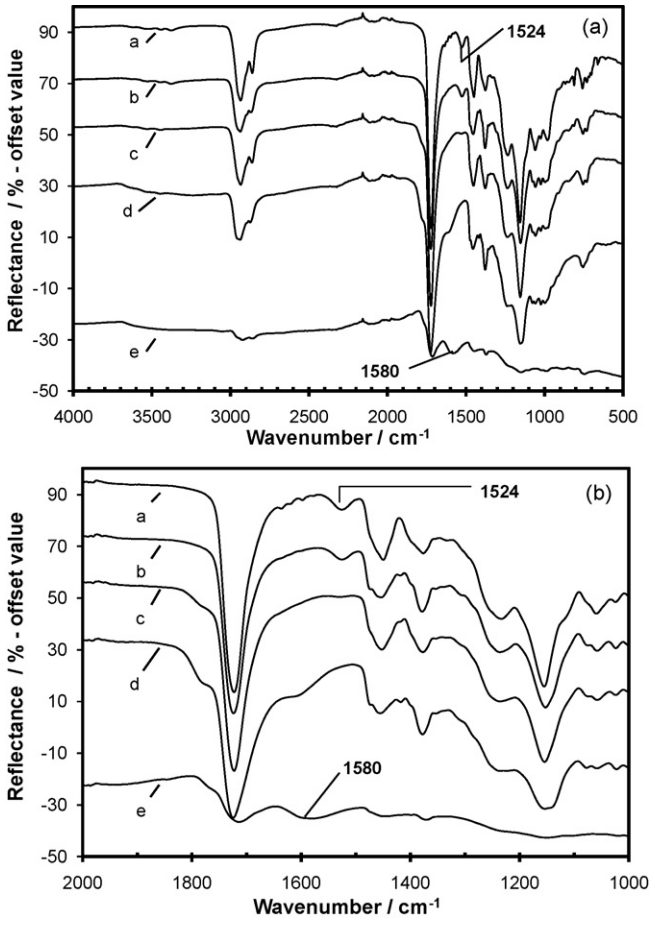


**Fig. 3.** (a) Infrared spectra (% reflectance ATR) of most crosslinked film (crosslink density = $1.7 \times 10^4$ mol m$^{-3}$): (A) not subjected to thermal degradation; (B) after 15 min at 300 °C in $N_2$ flow (data was offset by −20%); (C) after 90 min at 300 °C in $N_2$ flow (data was offset by 40%); (D) after 90 min at 400 °C in $N_2$ flow (data was offset by 60%); (E) after 10 °C/min ramp to 450 °C in $N_2$ flow (data was offset by 90%). (b) The same spectra, common scale.

volatile products formation [7]. Concentration of selected urethane diacrylate oligomer blend with polyester main chain, CN966B85, was the same in all resin formulations to ensure invariant contribution of non-acrylate degradation to an observed thermally induced weight loss. The molecular weight of oligomer portion of the blend, CN966, was ≈5500 [61(a)]. Thus, relative contribution of four urethane bridges per oligomer molecule to the thermally induced weight loss was low relative to that of ester groups. The ATR FTIR spectra of polymer films subjected to thermal degradation in nitrogen flow indicated that urethane linkage remained intact even after degradation resulting in 80% mass loss (Fig. 3). Indeed, absorbance at frequencies characteristic for urethane (1524 cm$^{-1}$ and 1580 cm$^{-1}$) remained almost constant. On the other hand, absorbance at frequencies corresponding to acrylates and esters (carbonyl C=O stretch at 1720 cm$^{-1}$, C–O stretch four bands 1140 cm$^{-1}$ to 1180 cm$^{-1}$, 1180 cm$^{-1}$ to 1280 cm$^{-1}$, etc. [61(b)]) gradually disappear with thermally induced degradation (Fig. 3). Mechanism of polyester degradation is similar to polyacrylates degradation mechanism and the same volatiles are formed [7]. Polyester contribution to thermally induced weigh loss should also be relatively low considering that concentration of oligomer was ≈0.04 M. Regardless, the same mobility restrictions at higher degree of crosslinking apply to ester and to acrylate degradation [7].

The crosslink density of the UV-cured polyacrylates was calculated using an expression based on Flory's rubber elasticity theory (Eq. (1), Table 2) [4–6,62].

$$\nu_e = \frac{E'}{3RT} \quad (1)$$

where $\nu_e$ (mol m$^{-3}$) is a molar concentration of crosslinks, $E'$ (Pa) is tensile storage modulus measured at the rubbery plateau, $R = 8.31$ J K$^{-1}$ mol$^{-1}$ is universal gas constant, and $T$ (K) is absolute temperature. Crosslink density derived using Eq. (1) ranged from ≈120 mol m$^{-3}$ to ≈17,000 mol m$^{-3}$ (Table 2). The kinetic rubber elasticity theory is not valid for high degrees of crosslinking, and Eq. (1) is valid for polymers with modulus in the range of $2 \times 10^6$ to $2 \times 10^8$ Pa. Eq. (1) yields underestimated crosslink densities for moduli, $E' \gg 2 \times 10^8$ Pa. Storage moduli of the polyurethane acry-

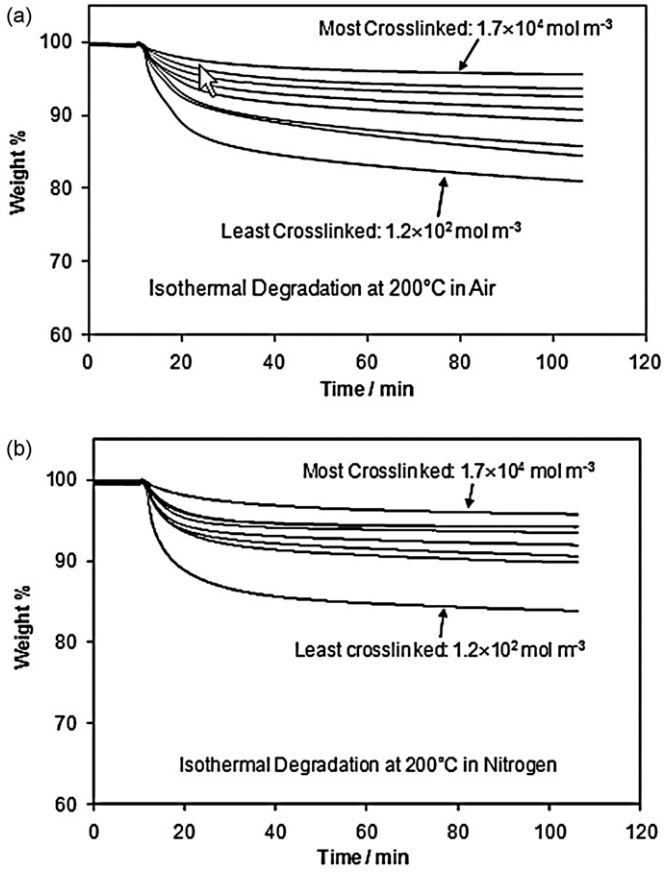


**Fig. 4.** Crosslink density effect on the kinetics of isothermal degradation of polyurethane acrylate films at 200 °C: (a) in air; (b) in nitrogen flow. The highest crosslink density was $1.7 \times 10^4$ mol m$^{-3}$, while the lowest was $1.2 \times 10^2$ mol m$^{-3}$ (Table 2).

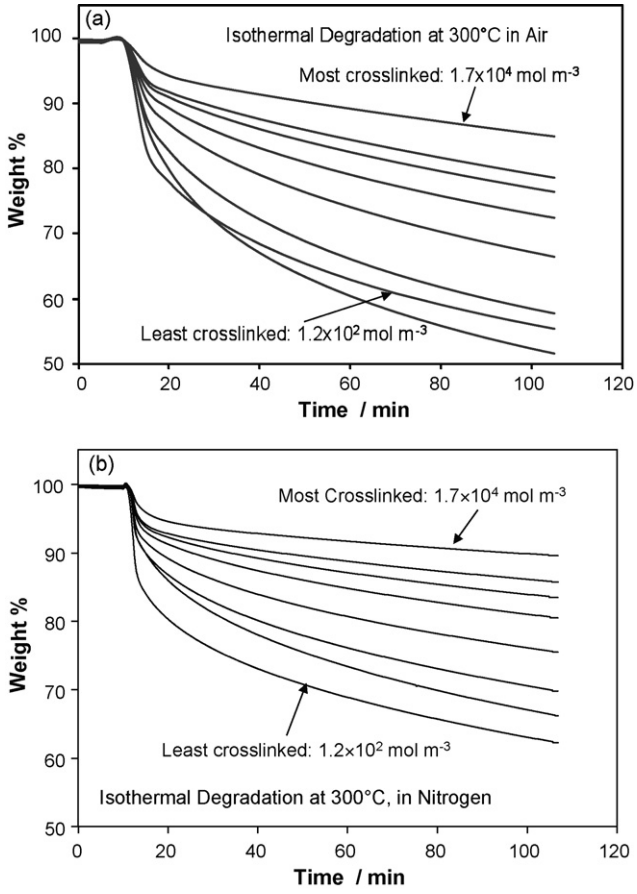


**Fig. 5.** Crosslink density effect on the kinetics of isothermal degradation of polyurethane acrylate films at 300°: (a) in air; (b) in nitrogen flow. The highest crosslink density was $1.7 \times 10^4$ mol m$^{-3}$, while the lowest was $1.2 \times 10^2$ mol m$^{-3}$ (Table 2).

lates studied here were close to the range in which the rubber elasticity theory (and Eq. (1)) is applicable.

Kinetics of isothermal degradation of polyurethane acrylates at each crosslink density was monitored in air and in nitrogen at 200 °C, 300 °C and 400 °C. Lower overall weight loss was observed in almost all the cases in acrylate films with higher crosslink density (Figs. 4–6).

Under temperature ramp (30–450 °C at 10 °C min$^{-1}$) polymers with higher crosslink density degraded faster above 400 °C in air and in nitrogen (Fig. 7), however initial onset of degradation (common term for the inflection point on a weight-loss curve describing TGA detected degradation kinetics) occurred at higher temperature in polymers with higher crosslink density (Fig. 8). Thus, an overall loss of weight in less crosslinked polymers was higher. The weight-loss-detected degradation kinetics was polychronal, for isothermal and temperature ramp conditions (Figs. 4–7) [1]. In non-isothermal process conducted in airflow, up to six stages could be identified (Fig. 2). When non-isothermal degradation kinetics was monitored in nitrogen flow, at most, four stages were observed. This occurred due to kinetic non-equivalence of reactive species in such non-uniform media as polymer solids [1]. Polychronal weight-loss kinetics observed by TGA could also be explained by multi-stage process yielding monomer and aldehydes in early stages of degradation and alcohols and water in later stages [31–34,39,63], carbon dioxide, and methanol in the early and late stages of degradation of acrylates [27–30,40,64]. The lower (initial) degradation onset temperatures increased with crosslink density. Higher onset temperatures were not dependent on crosslink density or the atmosphere at which thermal degradation was conducted (Fig. 8), in agreement with Emanuel and Buchachenko and Flory's statistical approach to polymer degradation, stating that kinetic non-equivalencies due to difference in chain segment mobility and environment are averaged at high degree of degradation and at high temperature, leading to monochronal degradation kinetics [1]. Such averaging occurred at all crosslink densities studied here (Fig. 8).

Thermo-oxidative degradation initiation involves peroxides formation, consequent formation of initiating PO$^{\bullet}$ radicals, reactions with P$^{\bullet}$ radicals and so on (Scheme 1) [1,7,24,46–48], in addition to hydrogen abstraction and valency migration through cyclization (Schemes 2 and 3) [1,7,24–45]. In the presence of oxygen (Schemes 1–3), formation of alcohol, water and carbon dioxide was expected to be faster than in the inert environment (Schemes 4 and 5), due to autocatalysis.

At all temperatures studied here difference in degradation kinetics in air and in nitrogen was substantially smaller than the difference resulting from the crosslink density change (Fig. 9). At 200 °C oxygen noticeably accelerated degradation of the least crosslinked polyacrylate (≈120 mol m$^{-3}$ of crosslinks). There was no detectable acceleration of the most crosslinked polyacrylate (≈17,000 mol m$^{-3}$ of crosslinks) degradation in the presence of oxygen (Fig. 9a). At 300 °C oxygen acceleration of the most crosslinked polyacrylate degradation became comparable to that of the least crosslinked one, with fasted degradation in air than in $N_2$ (Fig. 9b). At 400 °C an amount of weight loss in the absence of oxygen exceeded that in the presence of oxygen for all degrees of crosslinking (Fig. 9c). At 400 °C, the rate of weight loss in air was

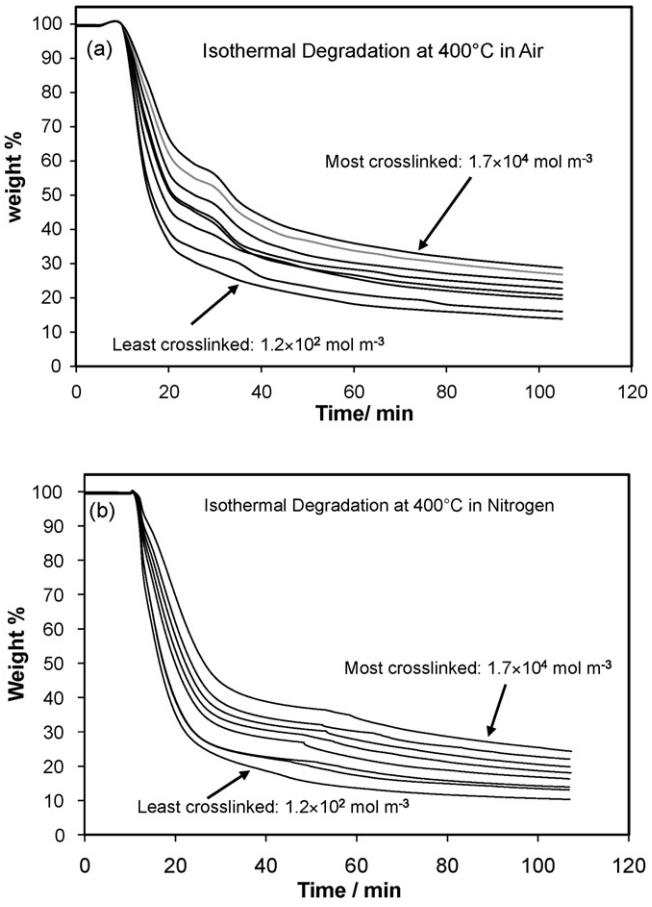


**Fig. 6.** Crosslink density effect on the kinetics of isothermal degradation of polyurethane acrylate films at 400°: (a) in air; (b) in nitrogen flow. The highest crosslink density was $1.7 \times 10^4$ mol m$^{-3}$, while the lowest was $1.2 \times 10^2$ mol m$^{-3}$ (Table 2).

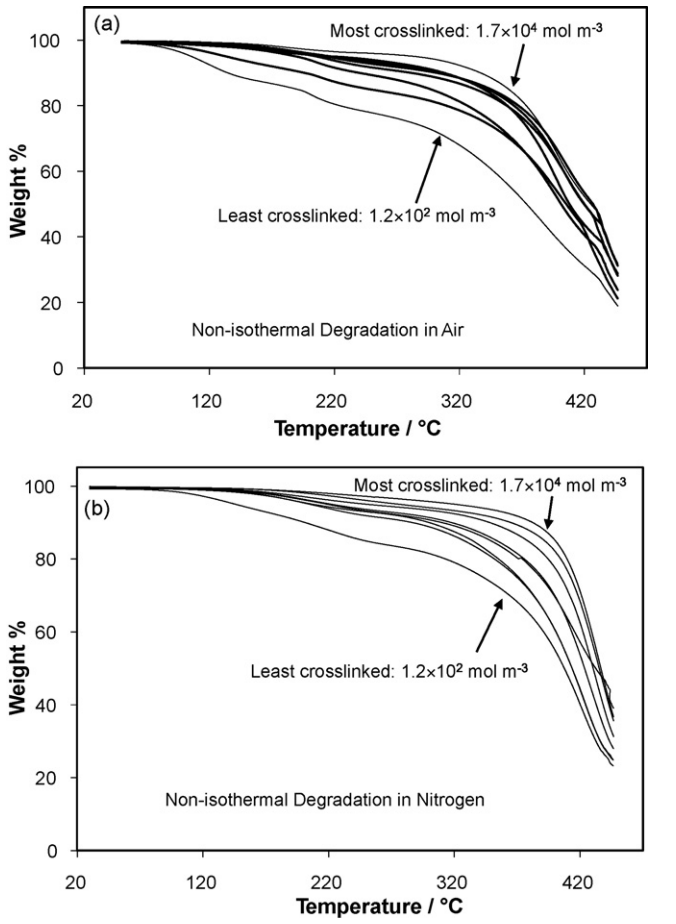


**Fig. 7.** Crosslink density effect on weight loss due to non-isothermal degradation of polyurethane acrylate films at (a) in air, (b) in nitrogen. Heating rate = 10 °C/min from 30 °C to 450 °C. The highest crosslink density was $1.7 \times 10^4$ mol m$^{-3}$, while the lowest was $1.2 \times 10^2$ mol m$^{-3}$ (Table 2).

slower than that in nitrogen atmosphere (Fig. 9c). These results were confirmed by temperature ramp experiments (Fig. 10).

The formation of peroxides would occur in the presence of oxygen however the weight-loss-detected degradation kinetics may be controlled not by oxygen diffusion rate but by other processes. Indeed, no crosslink density dependence of oxygen effects on radical life-time in photocrosslinked acrylates matrix was observed [41]. In addition, Kumins and Roteman reported that oxygen diffusion rate did not depend on glass transition temperature [3, p. 116]. Thus, crosslink density dependence of oxygen effects on degradation kinetics should be due to other factors than oxygen diffusion rate. Oxygen diffusivity in polymer matrix is $\geq 10^{-7}$ cm$^2$ s$^{-1}$, diffusivity of small molecules like alcohols, $\geq 10^{-9}$ cm$^2$ s$^{-1}$, while diffusivity of polymer segments is $\leq 10^{-10}$ cm$^2$ s$^{-1}$; these differences influence kinetics of radical reactions in polymer matrix [56,65–67] and kinetics of thermal degradation [1,2,7,24–45]. As will be shown below, oxygen diffusion rate will be higher than the rates of volatile products diffusion and rate of polymer segments motion. Temperature dependent diffusion coefficients make oxygen contribution to degradation kinetics difficult to predict, as was seen above (Fig. 9).

The mechanism of volatile products formation is similar with and without oxygen, since the same type of poly-radicals is formed (Schemes 2–5). If the volatile products formation and diffusion stages control the degradation rate, no or little difference between kinetics of degradation in the presence of oxygen and in nitrogen should have been observed. According to work of Grassie [31–34], Cameron [27–30], Haken [35(a)] and others [68,69] a majority of acrylate decomposition products are volatile. Haken emphasized formation of low volatility oligomer residue, however formation of substantial amounts of volatiles was detected: >40% of weight loss was reported to be due to monomer formation in the early stages and carbon dioxide in the later stages of degradation [35(b)]. Our dada confirmed these results and showed that degradation rates detected by the weight loss changed over the course of degradation (Figs. 4–7). The degradation rates were derived from experimental weight-loss kinetic curves (Figs. 4–7) at different degradation stages as $\Delta$(weight)/$\Delta$(time). The time intervals were selected at: 0–5 min, 0–10 min, 10–20 min, and 20–30 min. The derived degradation rates were plotted as a function of crosslink density (Figs. 11 and 12). Lower weight-loss rates observed at advanced stages of degradation (Figs. 11 and 12) were in agreement with observations of Lomakin et al. [37,38], Madorsky and Straus [68], Fourie and McGill [69], and Zislina et al. [70]. The rate of weight-loss decreased with crosslink density at all stages of degradation at 200 °C and 300 °C (Figs. 11a and b and 12a and b). At 400 °C the rate of weight loss at advanced degradation stage increased with crosslink density (Figs. 11c and 12c). Zislina et al. attributed similar observation to the catalysis of degradation by the products [70], while others considered polymer–substrate interference that did not exists in current work [69]. The reported decreased stability of highly crosslinked polymers [9] could have been an artifact resulting from the measurements conducted at the final stages of degradation at high temperature.

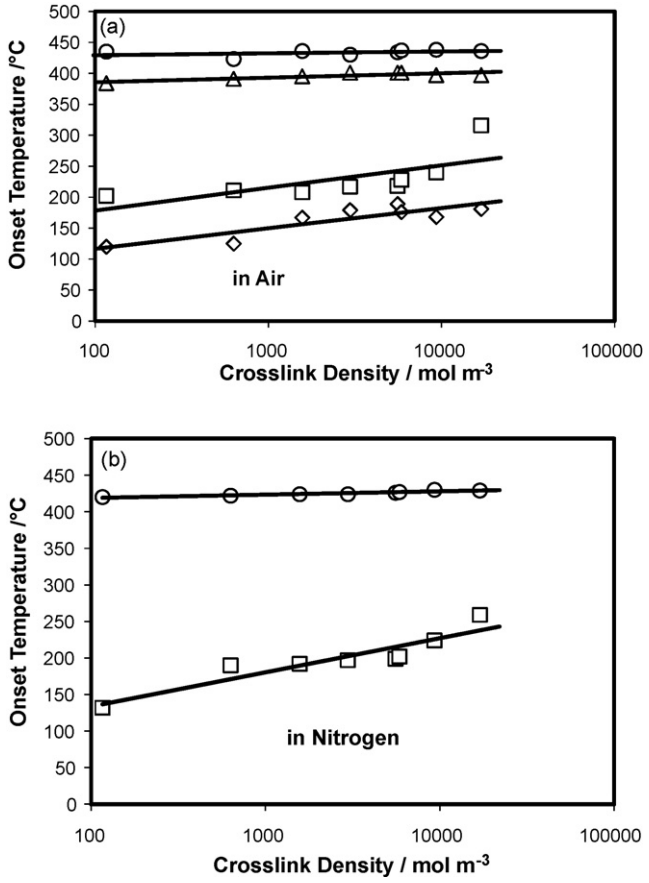


**Fig. 8.** Dependence of onset temperatures in non-isothermal degradation of photocrosslinked acrylates on crosslink density: (a) in air, (b) in nitrogen flow. Temperature ramp to 450 °C at 10 °C min$^{-1}$.

To ascertain a rate-controlling step of polyacrylate degradation, apparent activation energy, $E_a$, of initial stages of degradation was derived from the slope of the curves describing the initial rate (from 0 to 5 min) of the weight loss dependence on the inverse absolute temperature for each value of crosslink density (Figs. 13 and 14) [20–22]. As was emphasized by Emanuel et al. [1], polychronal degradation kinetics leads to multiple activation energies deduced at different temperature intervals (Figs. 13 and 14). The 200–300 °C Arrhenius slope yielded $E_a$ ranging from 12.6 kJ mol$^{-1}$ for lowest crosslink density (≈120 mol m$^{-3}$) to 25.1 kJ mol$^{-1}$ for highest crosslink density (≈17,000 mol m$^{-3}$). In 300–400 °C temperature interval $E_a$ ranging from 33.5 kJ mol$^{-1}$ to 58.6 kJ mol$^{-1}$ were obtained (Fig. 14). At 200–300 °C interval activation energies in the presence of oxygen were higher than those in nitrogen flow (Fig. 14b), while in the 300–400 °C oxygen presence lowered activation energies (Fig. 14a). Activation energies showed overall increase with increased crosslinked density. Similar values of $E_a$, from 23.5 to 80.0 kJ mol$^{-1}$, were reported for polyacrylates and polymethacrylates [8,71–73]. Values >84 kJ mol$^{-1}$ were reported elsewhere [38,45,74]. The temperature dependent $E_a$ was reported in the majority of publications [1,8,45,71–74].

Lomakin et al. concluded that relatively low activation energies indicated degradation kinetics controlled by the rate of volatile product diffusion [37,38]. Oxygen diffusion control of thermooxidation was often suggested as well [73]. However, almost no difference in rates of thermal degradation of polyacrylate samples of different thickness was found for thicknesses from 10 μm to 70 μm indicating that diffusion of oxygen and degradation products may not be the rate-controlling process in polymer degradation [37,75]. To verify the validity of Lomakin's conclusions, we monitored the kinetics of volatile products formation using mass-spectrometry. Mass values characteristic for carbon dioxide radical cation, M[$CO_2^{\bullet+}$]/$z$ = 44, and that of the acryloyl radical cation, M[$CH_2$=CH–C=O$^{\bullet+}$]/$z$ = 55, were most representative since these moieties are known to form in thermal degradation of higher polyacrylates and acrylic monomers [76,77]. Kinetics of volatile degradation products emission from most crosslinked (≈17,000 mol m$^{-3}$) and least crosslinked (≈120 mol m$^{-3}$) polyacrylates was monitored under temperature ramp to 450 °C at 10 °C min$^{-1}$ degradation (Fig. 15) and at constant temperatures of 200 °C and 300 °C (Fig. 16). Decarboxylation started at lower

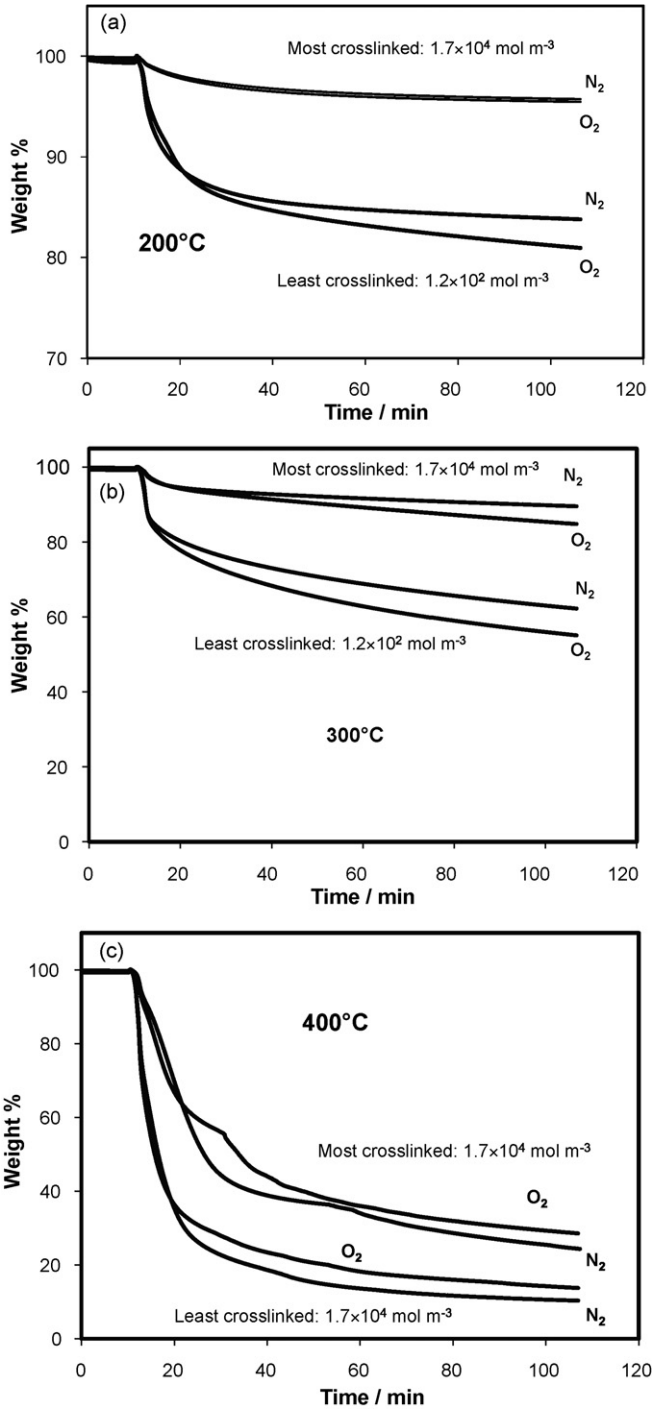


**Fig. 9.** Comparison of degradation kinetics in air and in nitrogen at (a) 200 °C, (b) 300 °C and (c) 400 °C. The highest crosslink density was 1.7 × 10$^4$ mol m$^{-3}$, while the lowest was 1.2 × 10$^2$ mol m$^{-3}$ (Table 2).

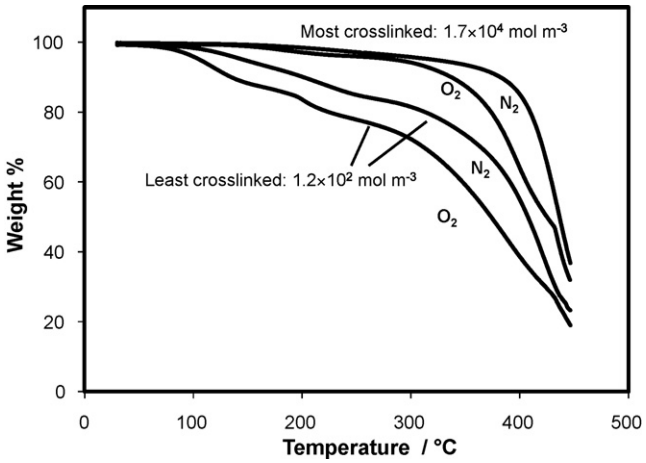


**Fig. 10.** Comparison of non-isothermal heating induced weight loss in most crosslinked and least crosslinked polyurethane acrylates in air and nitrogen flow. Temperature ramp to 450 °C at 10 °C min$^{-1}$. The highest crosslink density was $1.7 \times 10^4$ mol m$^{-3}$, while the lowest was $1.2 \times 10^2$ mol m$^{-3}$ (Table 2).

temperature for crosslink density of ≈120 mol m$^{-3}$ (Fig. 15). However, the maxima of $CO_2$ and monomer formation were observed at the same temperature (time) for most and least crosslinked polymer degradation in temperature ramp regime. In other words, no delay in $CO_2$ or monomer emission from polymer with crosslink density of ≈17,000 mol m$^{-3}$ relative to that of ≈120 mol m$^{-3}$ was observed at temperature ramp (Fig. 15). We did not detect a time lag between decarboxylation (detected by $CO_2$) and depolymerization (monitored by acryloyl radical cation) reported by Haken [35] and Lomakin et al. [37,38] neither at 300 °C (Fig. 16) nor at temperature ramp (Fig. 15) degradation. Higher mass volatile species (>80 a.u.) were detected at the same time as $CO_2$ and monomer, regardless of crosslink density.

At 200 °C kinetics of degradation products formation differed for most and least crosslinked polymers (Fig. 17). The $CO_2$ emission during the least crosslinked polymer degradation at 200 °C, passed through a maximum corresponding to maximum degradation rate similarly to those seen at 300 °C and at temperature ramp (Fig. 17a and b). During degradation of the least crosslinked polyacrylate at 200 °C the emission of $CO_2$ and monomer occurred at approximately same time (Fig. 17a and b). During the most crosslinked polymer degradation at 200 °C, no emission of monomer related ions or of higher molecular weight species were observed, and $CO_2$ emission amount increase did not exhibit maximum (Fig. 17a). The kinetics of $CO_2$ emission became identical as degradation of the most and least crosslinked polymer advanced, as expected from degradation induced chain length averaging [1,4]. The decarboxylation without monomer formation is consistent with degradation through a rotational diffusion of ester group to site of a radical (Schemes 4 and 5). The rotation of polymer segments is also consistent with low apparent activation energy of polyacrylate degradation and with an increase in activation energy with increase in crosslink density (Fig. 14). Change from degradation due to rotation of polymer segments at low temperature to a degradation through direct bond scission at higher temperatures may also explain increase in apparent activation energy with temperature. Absence of oxygen effects in most crosslinked polymer degradation at 200 °C (Fig. 9a) also indicated either restrictions of volatile products diffusion or hindrance of rotation required for decarboxylation among other products (Schemes 4 and 5). A possibility oxygen diffusion controlling faster degradation at higher temperature is discussed below.

If diffusion of volatile degradation products, such as $CO_2$, controlled crosslikned polyacrylate degradation kinetics as suggested

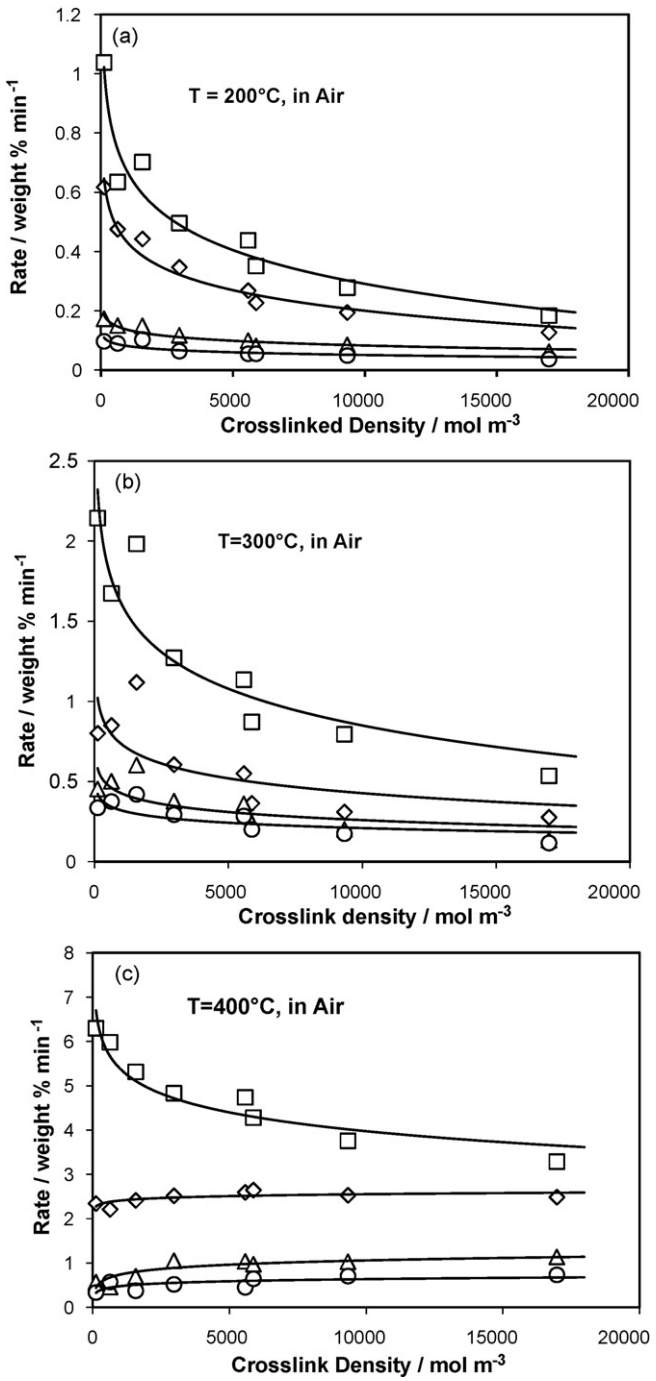


**Fig. 11.** Dependence of the thermal degradation rate of photocured urethane acrylate films on crosslink density in air: (a) at 200 °C, (b) at 300 °C, (c) at 400 °C. Rates were measured by the slope of the weight-loss kinetics curves (Fig. 2) at different stages of degradation, as Δ(weight)/Δ(time) at: (□) 0–5 min, (◊) 0–10 min, (△) 10–20 min, (○) 20–30 min.

by Lomakin et al. [37,38], degradation activation energy should be around or higher than 84 kJ mol$^{-1}$ [3] while $CO_2$ and acryloyl release time would differ in highly crosslinked polyacrylates degradation. This was not observed in the present work (Figs. 15 and 16). Higher molecular weight volatile products were also released without the time lag relative to $CO_2$ (Figs. 15 and 16). This again indicated that processes other than volatile products diffusion might be responsible for higher stability of highly crosslinked polymers.

Diffusion of carbon dioxide and monomer out of degrading polymers with highest and lowest crosslink density occurred with the same rate however, activation energy of the degradation is within

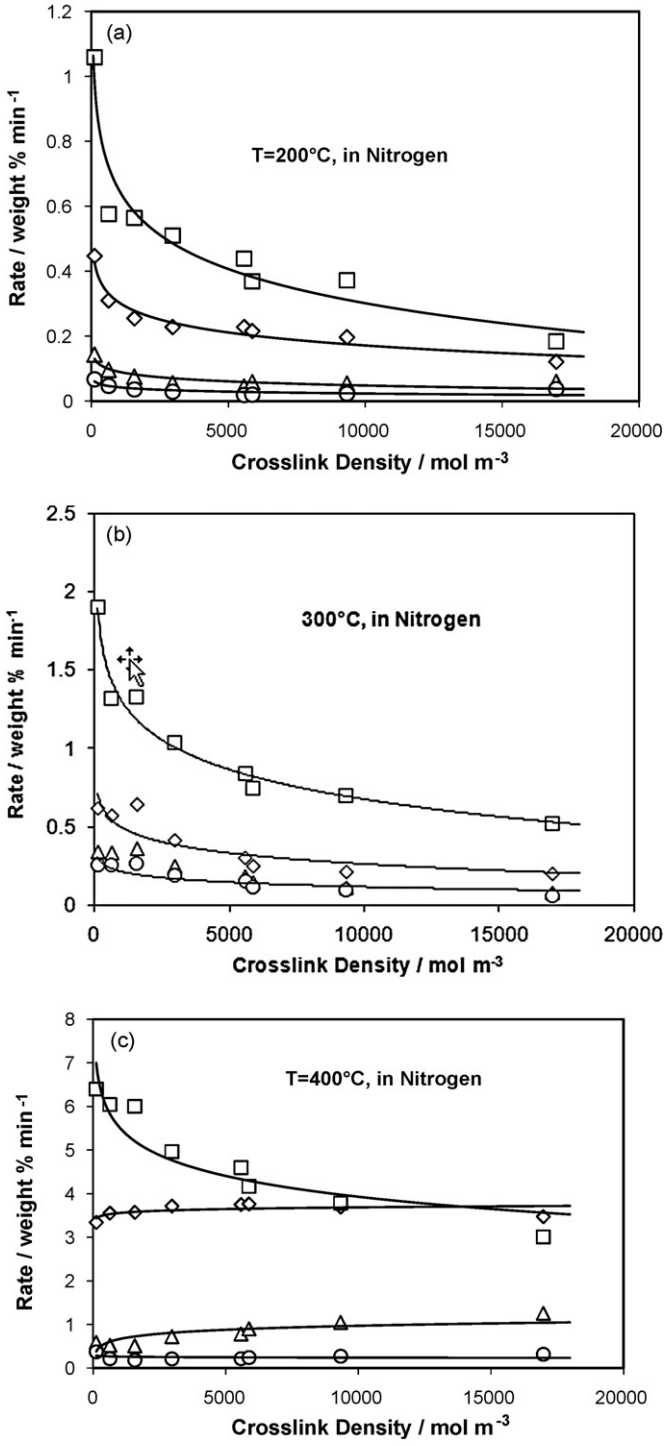


**Fig. 12.** Dependence of the thermal degradation rate of photocured urethane acrylate films on crosslink density in nitrogen flow: (a) at 200 °C, (b) at 300 °C, (c) at 400 °C. Rates were measured by the slope of the weight-loss kinetics curves (Fig. 2) at different stages of degradation, as Δ(weight)/Δ(time) at: (□) 0–5 min, (◊) 0–10 min, (△) 10–20 min, (○) 20–30 min.

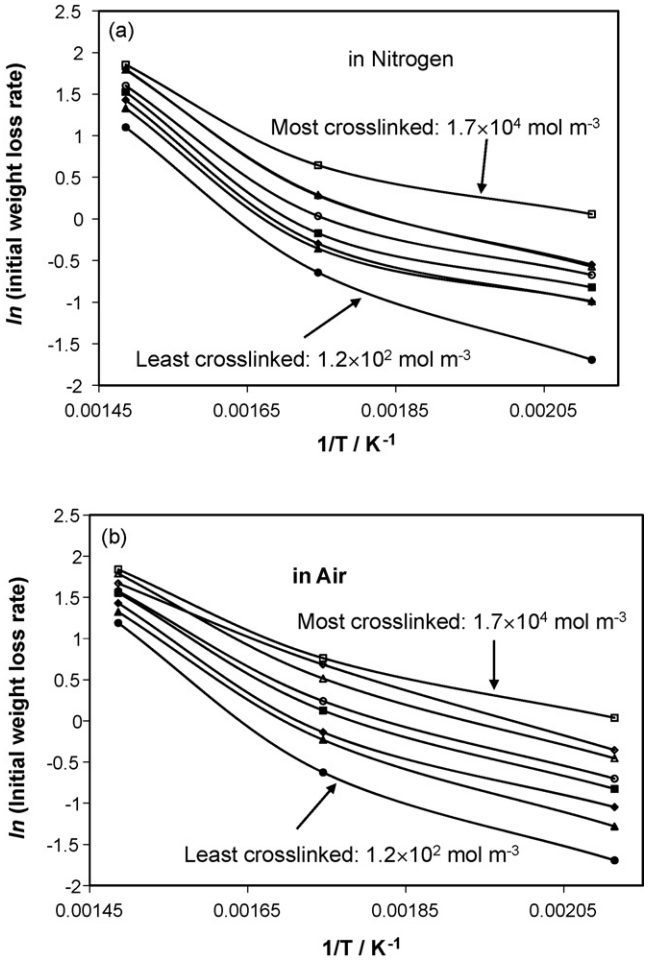


**Fig. 13.** Dependence of initial weight-loss rate (derived from the slope 0–5 min) on the inverse temperature (K): (a) in nitrogen, (b) in air. Crosslink densities (in mol m$^{-3}$) are (●) $1.2\times10^2$; (▲) $6.3\times10^2$; (♦) $15.7\times10^2$; (■) $29.7\times10^2$; (○) $55.8\times10^2$; (△) $58.8\times10^2$; (◊) $93.3\times10^2$; (□) $169.7\times10^2$.

the range corresponding to that of smaller molecules diffusion, and that of rotational diffusion of polymer segments in polymers above their glass transition temperature.

Diffusion of small molecules in polymers above their glass transition can be described by Eyring's transition state theory of rate processes [3,78,79]. The Eyring's approach is based on the model of liquid or polymer where holes of molecular size (free volume) are overwhelmingly abundant [80] and diffusion is stipulated by a random shift of the polymer segments to allow motion of penetrant [3,78–81]. Fox and Loshak derived the dependence of number of chain segments required for gas diffusion on apparent activation energy of this gas diffusion in polymer (Eq. (2)) [3, p. 120]:

$$\frac{Nf_c}{f_g} \cong \frac{\Delta E_d}{RT_g} \tag{2}$$

where $N$ is the number of polymer chain segments participating in small molecule diffusion, $\Delta E_d$ (J mol$^{-1}$) the diffusion threshold energy, $R = 8.31$(J K$^{-1}$ mol$^{-1}$) a universal gas constant, $T_g$ (K) the glass transition temperature, $f_c$ the critical fractional free volume required for segment to jump or move, and $f_g$ is the free volume fraction at glass transition temperature. If small molecule diffusion-controlled degradation is assumed, then using the apparent activation energy of degradation, measured as described above, the number of segments that should shift to permit such diffusion can be estimated (Eq. (2)). Thus for the highest activation energy corresponding to a most crosslinked polymer with $T_g = 65.2$ °C, considering that $f_c \approx 0.3$ [3 pp. 111, 117, 118], and maximum theoretical $f_g = 0.113$ [6 pp. 383, 82, 83], one obtains $N \approx 7.8$. For the least crosslinked polymer with $T_g = -48.7$ °C, one obtains $N \approx 6.7$. These values correspond to oxygen diffusion according to Kumins and Kwei [3, p. 118]. Thus, degradation threshold energies and number of moving chain segments in our most and least crosslinked acrylates are consistent with those of oxygen diffusion into polymer. Diffusion of polymer segments also occurs with

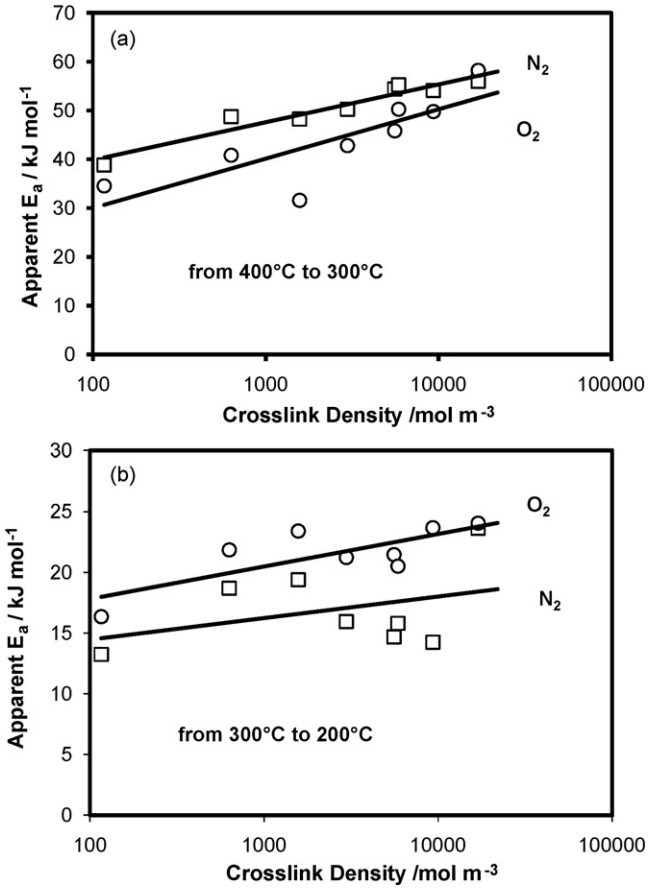


**Fig. 14.** Dependence of apparent activation energy of crosslinked polyurethane acrylates thermal degradation on crosslink density derived from the graphs of the degradation rate dependence on inverse temperature: (a) temperature interval from 300 °C to 400 °C, (b) temperature interval from 200 °C to 300 °C. (□) In nitrogen and (○) in air.

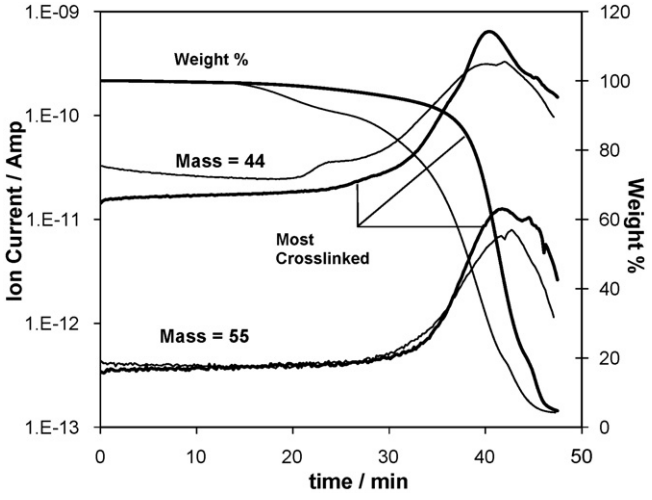


**Fig. 15.** TGA-Mass-spectrometry: kinetics of non-isothermal degradation of crosslinked polyurethane acrylates detected by carbon dioxide release (Mass = 44 a.u.) and by release of forming monomer (detected by acryloyl radical cation, Mass = 55 a.u.). Nitrogen flow. Thicker lines correspond to most crosslinked polymer.

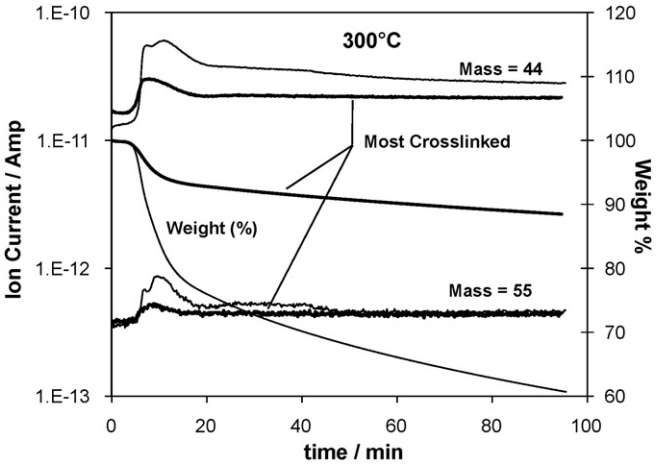


**Fig. 16.** TGA-Mass-spectrometry: kinetics of 300 °C isothermal degradation of crosslinked polyurethane acrylates detected by carbon dioxide release (Mass = 44 a.u.) and by release of forming monomer (detected by acryloyl radical cation Mass = 55 a.u.). Nitrogen flow. Thicker lines correspond to the most crosslinked polymer.

$\Delta E_d \approx 24.3\,\mathrm{kJ\,mol^{-1}}$ activation energy [3]. The ≈7 chain segments are also sufficient for cyclic decarboxylation. So oxygen diffusion and decarboxylation control of degradation kinetics cannot be elucidated. The crosslink density stipulated thermal stability increase was observed in the absence of oxygen as well, raising a question of oxygen diffusion control of kinetics of polymer thermal degradation. The above results did not exclude kinetics controlled by carbon dioxide and other volatile products diffusion out of polymer matrix [37,38].

The diffusion rate depends on molecular structure (collisional crossections, Van der Waals potentials, etc.) of the diffusing molecules [21,22,78] and polymer glass transition temperature [3,78, 83 and ref. therein]. Eyring's temperate dependence is observed as well:

$$D = D_0 \exp\left(\frac{E_D}{RT}\right) \tag{3}$$

$$\left(\frac{\sigma_{N_2}}{\sigma_X}\right)^2 \times 10^{-3}\frac{E_D}{R} = 7.5 - 2.5 \times 10^{-4}(298 - T_g)^2 \quad \text{for } T_g < 298\,\mathrm{K} \tag{4}$$

$$\left(\frac{\sigma_{N_2}}{\sigma_X}\right)^2 \times 10^{-3}\frac{E_D}{R} = 7.5 - 2.5 \times 10^{-4}(298 - T_g)^{3/2} \quad \text{for } T_g > 298\,\mathrm{K} \tag{5}$$

$$\log D_0 = \frac{E_D \times 10^{-3}}{R} - 4.0 \quad \text{for } T_g < 298\,\mathrm{K} \tag{6}$$

$$\log D_0 = \frac{E_D \times 10^{-3}}{R} - 5.0 \quad \text{for } T_g > 298\,\mathrm{K} \tag{7}$$

$$\log D(T) = \log D_0 - \frac{435 \times 10^{-3} \times E_D}{T \times R} \quad \text{overall } D \text{ approximation at any } T \tag{8}$$

where $E_D$ is an apparent activation energy of diffusion, $\sigma_X$ is collisional cross-section diameter of the diffusing molecule, $X$, $D$ and $D_0$ are diffusion coefficient and pre-exponential term in Eq. (3) [3,83]. Following Van Krevelen [83], and Herschfelder et al. [78] $\sigma_{CO_2} = 39.4\,\text{Å}$, $\sigma_{O_2} = 34.7\,\text{Å}$, $\sigma_{N_2} = 38.0\,\text{Å}$. The following results were obtained using Eqs. (6)–(11) (Table 3) [83, pp. 546–583]. The

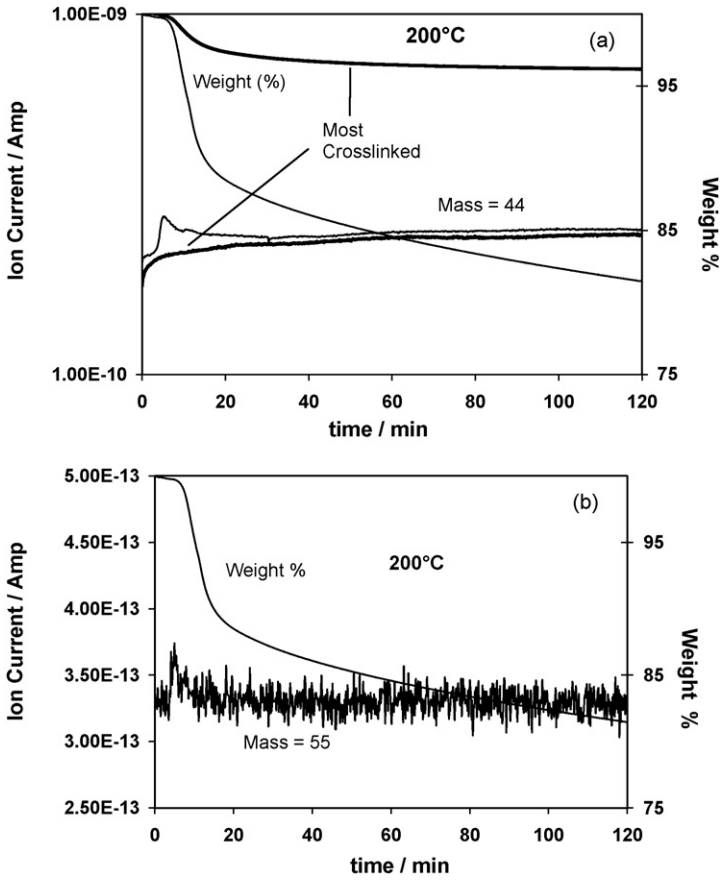


**Fig. 17.** TGA-Mass-spectrometry: kinetics of 200 °C isothermal degradation of crosslinked polyurethane acrylates detected by carbon dioxide release (Mass = 44 a.u.) and by release of forming monomer (detected by acryloyl radical cation Mass = 55 a.u.). Nitrogen flow. (a) Least crosslinked polymer sample; (b) most crosslinked polymer sample.

"compensation effect" of higher $D_0$ values reduces the influence of higher threshold energy $E_D$ in diffusion coefficient computations. This results at higher temperature in computed $CO_2$ diffusivities being higher than computed $O_2$ diffusivities (Table 3) [83]. The values of computed activation energies are close to those measured in this work.

Activation energy of products diffusion is close to that of rotational diffusion of polymer chain segments [84]. Computed diffusion coefficients can be used to estimate the rates of reactions controlled by oxygen or carbon dioxide diffusion using Smoluchowski equation [20,21,56,65,85] (Eq. (9)):

$$k_{diff} = 2\pi D_{AB}(\sigma_A + \sigma_B)N_A \approx 4 \times 10^{14} D_{AB} \quad (9)$$

The computed rate constants range from $7 \times 10^9$ l mol$^{-1}$ s$^{-1}$ to $6 \times 10^{10}$ l mol$^{-1}$ s$^{-1}$ for $CO_2$ diffusion control and from $5 \times 10^{11}$ l mol$^{-1}$ s$^{-1}$ to $3 \times 10^{12}$ l mol$^{-1}$ s$^{-1}$ for $O_2$ diffusion control.

Such high rate constants are encountered in radical reactions in solution, fluorescence emission decay. Thus, approximate calculations using Eqs. (3)–(9) indicate that thermal degradation kinetics control by oxygen or carbon dioxide diffusion is unlikely. Even if diffusing molecule cross-section would be 10-fold higher to account for larger molecules formation, the diffusion control would require degradation kinetics to occur with the rates corresponding to extremely fast processes that are not known to participate in thermal degradation.

Another approach to evaluating whether the diffusion of gasses in or out of degrading acrylates can control weight-loss kinetics can be used as well. Using computed diffusion coefficients one can estimate time required for $O_2$ and $CO_2$ molecules to diffuse through a film thickness during thermal degradation. A simplified time-lag approximation to solution of diffusion equation suffices (Eq. (10)) [3]:

$$t = \frac{l^2}{6D} \quad (10)$$

where $t$ is the time required for a molecule of diffusivity, $D$, to diffuse through thickness $l$. For $l \approx 75$ μm and $D \approx 10^{-5}$ cm$^{-2}$ s$^{-1}$ (lowest diffusivities at 200 °C, Table 3), $t \approx 0.9$ s, and for $D \approx 10^{-3}$ cm$^2$ s$^{-1}$ (lowest diffusivities at 400 °C, Table 3), $t \approx 0.009$ s. Thus, diffu-

**Table 3**
Computed diffusivities and diffusion threshold energies.

| Temperature | Diffusing specie | $D$ (cm$^2$ s$^{-1}$) | | Computed $E_D$ (kJ mol$^{-1}$) | Smoluchowski's rate constant (l mol$^{-1}$ s$^{-1}$) | |
|---|---|---|---|---|---|---|
| | | 200 °C | 400 °C | | 200 °C | 400 °C |
| Most crosslinked ($T_g$ = 338.2 K) | $CO_2$ | $4.12 \times 10^{-5}$ | $5.5 \times 10^{-3}$ | 63.6 | $8.2 \times 10^9$ | $1.1 \times 10^{12}$ |
| | $O_2$ | $3.5 \times 10^{-5}$ | $2.5 \times 10^{-3}$ | 56.5 | $7.0 \times 10^9$ | $5.0 \times 10^{11}$ |
| Least crosslinked ($T_g$ = 224.3 K) | $CO_2$ | $3.2 \times 10^{-4}$ | $1.7 \times 10^{-2}$ | 52.6 | $6.4 \times 10^{10}$ | $3.4 \times 10^{12}$ |
| | $O_2$ | $2.8 \times 10^{-4}$ | $9.4 \times 10^{-3}$ | 46.4 | $5.6 \times 10^{10}$ | $1.9 \times 10^{12}$ |

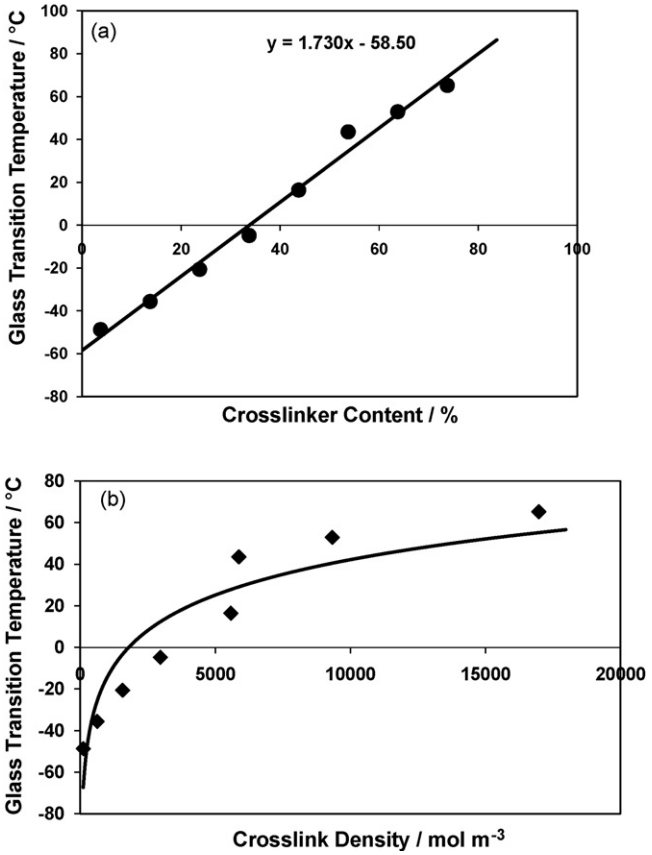


**Fig. 18.** Dependence of glass transition temperature on total diacrylate moieties concentration in the resin formulation (a) and on derived crosslink density (b).

sion of oxygen and carbon dioxide may play role in degradation kinetics control at 200 °C, but diffusion rates appear too high to control observed degradation kinetics at 400 °C. For $CO_2$ the above results diverge (at least at temperatures >200 °C) from Lomakin's conclusion that products diffusion controls thermal degradation kinetics [37,38]. However, diffusion of larger fragments and acrylic monomer out of degrading polyacrylate can control the degradation kinetics as Lomakin suggested. The kinetic control by slower movement of chain segments in degrading polymer solid (diffusivities as low as $10^{-11}$ $cm^2$ $s^{-1}$ [3,5,6]) with consequent formation of cyclic intermediate may be a plausible degradation rate-controlling step, as discussed below.

The length of polymer fragments available for rearrangement can be estimated based on glass transition and rubber elasticity theory. However, quantitative relations between polymer glass transition temperature and crosslink density are not fully established. One of the reasons is deviation of polymer behavior at high crosslink density from that predicted by rubber elasticity theory [86–93]. The theory used to derive Eq. (1) is applicable in limited the range of elastic storage modulus, $2 \times 10^6$ Pa < $E'$ < $2 \times 10^8$ Pa [82,86–93]. Although storage modulus of photocrosslinked polyurethane acrylates used in the current study was within these limits (Table 2), and glass transition temperature depended linearly on difunctional species concentration (Fig. 18a), glass transition temperature dependence on crosslink density computed by Eq. (1) deviated from linearity (Fig. 18b). Similar crosslinked polyacrylates behavior was reported and analyzed by Tobolsky et al. [88]. To avoid rubber elasticity considerations, semi-empirical equations can be used to derive molecular properties of the highly crosslinked polymers.

The polymer structure may be elucidated to some extend using Nielsen equation that relates glass transition temperature to concentration of elastic chains [86]:

$$T_g = T_{g_0} + \frac{3.9 \times 10^4}{\overline{M_c}} \tag{11}$$

where $T_g$ is crosslinked polymer glass transition temperature, $T_{g_0}$ is glass transition temperature of the polymer in non-crosslinked limit, $\overline{M_c}$ is number average molecular weight of the polymer chains between the crosslinks [86,88,93]. Glass transition in our most crosslinked polymer occurs at ≈65.2 °C and in the least crosslinked polymer at ≈−48.7 °C (Fig. 1b and Table 2). Linear extrapolation to 0% concentration of difunctional species yields $T_{g_0} \approx -60$ °C (Fig. 18). Therefore, for most crosslinked polymer studied here $\overline{M_c} \approx 312$ g mol$^{-1}$ and for the least crosslinked, $\overline{M_c} \approx 3450$ g mol$^{-1}$ (Eq. (3)). Eq. (11) and similar expressions [86–88] are only approximate, however an order of magnitude difference in estimated chain length should lead to noticeable difference in chain segments mobility. An average number of atoms in polymer backbone between the crosslinks, $\bar{n}_c$, can be approximated (Eq. (12)) [86]:

$$T_g = T_{g_0} + \frac{788}{\bar{n}_c} \tag{12}$$

Using Eq. (12) $\bar{n}_c \approx 70$ atoms crosslink$^{-1}$ for the least crosslinked polyacrylate and $\bar{n}_c \approx 6.3$ atoms crosslink$^{-1}$ for the most crosslinked polyacrylate was found. Comparing $\overline{M_c}$ and $\bar{n}_c$ (Eqs. (11) and (12)), we obtain for a molecular weight of the repeating unit between crosslinks to be $\bar{M}_{rep} \approx 50$ g mol$^{-1}$. This would be a reasonably close number for acrylic derivatives (Schemes 2–5).

Segmental mobility in network with 6 atoms in polymer backbone between the crosslink should be lower than in one with 70 atoms. However the number of atoms in the backbone, $\bar{n}_c \approx 6$, is sufficiently large to allow oxygen and carbon dioxide diffusion to be comparable at both levels of crosslinking, as indicated by Eyring diffusion theory and Eq. (2).

Rotational degrees of freedom that control decarboxylation and degradation rates (Schemes 4 and 5), can be found using approach of Bicerano, who related glass transition temperature to chain segments mobility (Eq. (5)) [89]:

$$T_g = T_{g_0} + \frac{T_{g_0} \times const}{n \times N_{rot}} \tag{13}$$

where $n = \overline{M_c}/\bar{M}_{rep}$, $\bar{M}_{rep}$ is the molecular weight per repeat unit and $N_{rot}$ is the rotational degrees of freedom parameter quantifying chain flexibility [89]. Product $n \times N_{rot}$ corresponds to average number of rotational degrees of freedom between crosslinks. Bicerano's interpretation shows that the number of rotational degrees of freedom in chains between crosslinks is >10 times lower in the most crosslinked polyurethane acrylate than in the least crosslinked polyurethane acrylate studied here (Eq. (13), Table 2). Although the results of the above computations do not exclude reduction of diffusion rate of $CO_2$ and other volatile products with increase in crosslink density, the considerations of activation energy and segment mobility change presented above indicated rotational diffusion-controlled decarboxylation and monomer formation may control the kinetics of studied polyurethane acrylates degradation. In other words, diffusion of $CO_2$ and other volatile products out of degrading crosslinked acrylates would occur faster than rotational diffusion of the polymer chain segments required for formation of cyclic transition state, preceding the formation of these products (Schemes 4 and 5).

The cyclization (loop closure) time, $\tau_c$, in polymers can also be deduced using the Kargin–Slonimskii–Rouse-type approach for non-interacting chain segments motion, derived for polymer solu-

tion but applicable to motion in matrix [5,94–97].

$$\tau_c \approx \frac{b^3}{D_0} N^{\alpha} \qquad (13')$$

where $b$ is monomer segment length, $D_0$ is monomer segment diffusivity, $N$ is the chain fragment length and $\alpha$ is 3/2 or 2 depending on the polymer model used [94–97]. In other words, the rate constant for decarboxylation intermediate cycle formation, $k = 1/\tau$ [79] is proportional to monomer diffusion rate [97,98]. The number of chain segments required for cyclization, $N$, remains constant. The monomer segment diffusivity, $D_0$, decrease with crosslink density increase ensures that cyclization and consequent degradation will be slower in polymers with higher crosslink density. The problem of differentiating kinetics control stipulated by forming products escape rate from that of cyclization remains in the absence of detailed numerical analysis. It is however informative that no difference in the rate of emission of monomer and carbon dioxide was detected by TG-MS and no sample thickness effects on polyacrylate degradation rate were detected.

Generalized kinetic modeling of polymer degradation in solution also indicated that polymer stability increase with increase of crosslink density is to be expected [99–101]. Results and numerical estimation presented above indicated that straightforward control of thermal degradation kinetics by the rate of oxygen uptake and carbon dioxide and other volatile products diffusion rates in polymer matrix [52,93] does not explain all the observations. It is likely that the degradation kinetics is controlled by the rate of polymer segment rotation leading to decarboxylation and formation of low molecular weight species.

Chain initiation often defines degradation rate (Scheme 1) [1,7,24,46–48,85]. Radical pair formation upon thermal activation is reversible and radical pair must move out of the cage and be stabilized to initiate chain degradation [85]. The separation of radicals is diffusion controlled and probability of escape from the cage after radical pair formation decreases with radicals and chain segments diffusivity decrease [85]. The radical recombination in cage is collision-controlled ($k \sim 10^{13}\ s^{-1}$). Although sterric restrictions lower radicals recombination rate to allow radicals escape from the cage [85,56,102], diffusion coefficients decrease with crosslink density (Table 3) will also be consistent with lower degradation rate at higher polymer crosslinking. The activation energy of radical escape from the cage is close to that found in the present work. In case of chain scission leading to two high molecular weight fragments, the radical-bearing chain ends must separate by rotational diffusion of polymer segments in matrix (Eq. (13)). Obviously, lower rotational diffusivity will result in lower probability of cage escape. More quantitative approaches may be sought. Detailed numerical modeling [56,65,99–102] of the degradation kinetics lies outside the scope of this work, however a semi-quantitative use of the available segments mobility models indicated degradation kinetics may be controlled by the rate of rotational diffusion of polymer chain segments.

## 4. Conclusion

A series of photocrosslinked poly(urethane acrylates) with increasing crosslink densities and glass transition temperatures ranging from −48.7 °C and +65.2 °C was designed and formulated to analyze the effects of crosslink density on thermal stability of polymers. Crosslink density and glass transition temperatures were derived using dynamic mechanical analysis. The kinetics of photocrosslinked poly(urethane acrylates) thermal degradation was monitored by the loss of volatile products detected by TGA and TGA-Mass-spectrometry at temperatures 100–450 °C. The rate of early stages of degradation, <5 min from the beginning, decreased with the increase of crosslink density. No time lag between elution of carbon dioxide and that of acrylate monomers was observed by TG-MS. At 400 °C and above, the rate of volatiles loss increased with crosslink density at longer times (10–15 min after the beginning of degradation). This may explain, why decreased stability at higher crosslinking was sometimes reported [9,11].

Degradation onset temperatures and apparent activation energies of volatiles loss increased with increased crosslink density. The values of apparent activation energies ranged from ≈13 kJ mol$^{-1}$ to ≈63 kJ mol$^{-1}$. Such activation energies were computed to correspond to motion of 7–8 polymer chain segments, under small molecule diffusion assumption. This number of chain segments was sufficient for oxygen diffusion, but was less than what is required for $CO_2$ and monomer molecules diffusion. Diffusion coefficient computations also yielded diffusivities too high to control the rate of observed degradation kinetics. The observed data, however are consistent with degradation rate controlled by rotational diffusion of chain segments required for cyclic decarboxylation (Schemes 4 and 5) and stabilization of polymeric radicals.

Although complete separation of processes controlled by small molecules diffusion and those controlled by chain segment mobility is rather problematic, all the data on increase of polymer stability with increase of crosslink density could be explained in a straightforward way by reduction in the chain segment mobility, since the motion of segments is required for small molecules diffusion as well as for formation of cyclic transition state. Further experimental and computational investigations are necessary to get unequivocal answer on correlation of degradation kinetics with polymer structure.

Use of classic methods of thermogravimetric analysis allowed direct monitoring of polyacrylate degradation processes and straightforward data interpretation.

## References


[1] E.M. Emanuel, A.L. Buchachenko, C.R.H. de Jonge (Eds.), Chemical Physics of Polymer Degradation and Stabilization, New Concepts in Polymer Science Series, VNU Science Press, Utrecht, Netherlands, 1987.
[2] A.S. Kuz'minskii (Ed.), The Ageing and Stabilization of Polymers, Elsevier, Amsterdam, London, New York, 1971.
[3] J. Crank, G.S. Park (Eds.), Diffusion in Polymers, Academic Press, New York, 1968.
[4] P.J. Flory, Principles of Polymer Chemistry, Ithaca Cornell University Press, New York, 1953.
[5] M. Rubinstein, R.H. Colby, Polymer Physics, Oxford University Press, New York, 2006.
[6] L.H. Sperling, Introduction to Physical Polymer Science, 4th ed., John Wiley & Sons, Hoboken, New Jersey, 2006.
[7] R.T. Conley, in: R.T. Conley (Ed.), Thermal Stability of Polymers, vol. 1, Marcel Dekker, Inc., New York, 1970.
[8] M. Kryszewski, Pure Appl. Chem. 51 (1979) 2395.
[9] R.G. Sousa, W.F. Magalhaes, R.F.S. Freitas, Polym. Degrad. Stabil. 61 (1998) 275.
[10] (a) L.P. Smirnov, N.N. Volkova, Prog. Colloid Polym. Sci. 90 (1992) 222;
(b) P. Thavamani, A.K. Sen, D. Khastgir, A.K. Bhowmick, Thermochim. Acta 21 (1993) 293.
[11] A. Lee, G.B. McKena, Polymer 29 (1988) 1812.
[12] L. Slusarski, G.J. Janowska, J. Therm. Anal. 29 (1984) 95.
[13] A.S. Lukin, Z.N. Tarasova, B.A. Dogadkin, Kolloidnyi Zhurnal 27 (2) (1965) 224.
[14] K. Ono, A. Kaeriyama, K. Murakami, J. Polym. Sci. Polym. Chem. 13 (11) (1975) 2615;
K. Ono, A. Kaeriyama, K. Murakami, J. Polym. Sci. Polym. Chem. 16 (7) (1978) 1575;
K. Ono, A. Kaeriyama, K. Murakami, Nippon Gomu Kyokashi 51 (1) (1978) 52;
K. Ono, A. Kaeriyama, K. Murakami, Nihon Reoroji Gakkaishi 7 (2) (1979) 51.
[15] N.N. Volkova, U.A. Ol'hov, S.M. Baturin, Vysokomol. Soedin. Ser. A 20 (1) (1978) 199.
[16] N.L. Panteleeva, E.A. Il'ina, S.M. Kavun, Vysokomol. Soedin. Ser. B: Kratkie Soobsh 28 (6) (1986) 474.
[17] B.V. Erofeev, Dokl. Acad. Nauk SSSR 52 (6) (1946) 515.
[18] V.V. Korshak, G.M. Tsetlin, V.N. Ryzhov, Dokl. Acad. Nauk SSSR 293 (4) (1987) 903.
[19] Yu.I. Matsusevich, L.P. Krul, Plastich. Massy 3 (1991) 11.
[20] P.W. Atkins, Physical Chemistry, W.H. Freeman & Co., San Francisco, 1978;
H. Eyring, J. Chem. Phys. 4 (1936) 283.

[21] P.J. Robinson, K.A. Holbrook, Unimolecular Reactions, 1st ed., Wiley–Interscience, New York, NY, 1972.
[22] V.V. Krongauz, B.S. Rabinovitch, Chem. Phys. 47 (1980) 9;
V.V. Krongauz, B.S. Rabinovitch, Chem. Phys. 67 (1982) 201;
V.V. Krongauz, B.S. Rabinovitch, J. Chem. Phys. 78 (6) (1983) 3872;
V.V. Krongauz, B.S. Rabinovitch, J. Chem. Phys. 78 (9) (1983) 5643.
[23] H.A. Schneider, Polym. Eng. Sci 32 (17) (1992) 1309;
H.A. Schneider, J. Therm. Anal. 40 (2) (1993) 677;
H.A. Schneider, Thermochim. Acta 83 (1) (1985) 59;
H.A. Schneider, Polym. Bull. (Germany) 2 (8) (1980) 551.
[24] E.T. Denisov, Russ. Chem. Rev. (Uspekhi Khimii) 47 (6) (1978) 572.
[25] A. Votinov, P. Kobeko, F. Marei, J. Phys. Chem. (USSR) 16 (1942) 106.
[26] S.L. Madorsky, J. Polym. Sci. 11 (1953) 491.
[27] G.G. Cameron, D.R. Kane, J. Polym. Sci. 2B (1964) 693;
G.G. Cameron, D.R. Kane, Makromol. Chem. 109 (1967) 194;
G.G. Cameron, D.R. Kane, Makromol. Chem. 113 (1968) 75;
G.G. Cameron, D.R. Kane, Polymer 9 (9) (1968) 461.
[28] G.G. Cameron, F. Davie, D.R. Kane, Makromol. Chem. 135 (1970) 137.
[29] G.G. Cameron, F. Davie, Makromol. Chem. 149 (1971) 169;
G.G. Cameron, F. Davie, Chem. Zvesti 26 (3) (1972) 200.
[30] A.T. Bullock, G.G. Cameron, V. Krajewski, J. Phys. Chem. 80 (16) (1976) 1792.
[31] N. Grassie, B.J.D. Torrance, J. Polym. Sci. Polym. Chem. 6 (12) (1968) 3303, 3315.
[32] N. Grassie, J.G. Speakman, J. Polym. Sci. Polym. Chem. 9 (4) (1971) 949, 931.
[33] N. Grassie, Pure Appl. Chem. 30 (1–2) (1972) 119;
N. Grassie, Pure Appl. Chem. 34 (2) (1973) 247;
N. Grassie, Pure Appl. Chem. 54 (2) (1982) 337.
[34] N. Grassie, J.D. Fortune, Makromol. Chem. 162 (1972) 93;
N. Grassie, J.D. Fortune, Makromol. Chem. 168 (1973) 1, 13;
N. Grassie, J.D. Fortune, Makromol. Chem. 169 (1973) 117.
[35] (a) J.K. Haken, T.R. McKay, Anal. Chem. 45 (1973) 1251;
(b) J.K. Haken, L. Tan, J. Polym. Sci. Polum. Chem. 26 (5) (1988) 1315.
[36] T. Kashiwagi, A. Inabi, Polym. Degrad. Stabil. 26 (1989) 161.
[37] S.M. Lomakin, J.E. Brown, R.S. Breese, M.R. Nyden, Polym. Degrad. Stabil. 41 (1993) 229.
[38] S.M. Lomakin, R.M. Aseevea, G.E. Zaikov, Int. J. Polym. Mater. 31 (1–4) (1996) 153.
[39] R.S. Lehrle, E.J. Place, J. Polym. Degrad. Stabil. 56 (1997) 215, 221;
R.S. Lehrle, E.J. Place, J. Polym. Degrad. Stabil. 57 (1997) 247.
[40] B.A. Howell, B. Pan, Thermochim. Acta 357–358 (2000) 119.
[41] J. Pavlinec, N. Moszner, J. Placek, Macromol. Chem. Phys. 202 (2001) 2387.
[42] J.P. Chen, T. Kodaira, K. Isa, T. Senda, J. Mass Spectr. Soc. Jpn. 49 (20) (2001) 41.
[43] N.S. Allen, Photochemistry, vol. 34, The Roy. Soc. Chem., 2003, p. 197.
[44] F. Bertini, G. Audisio, V. Zuev, Polym. Degrad. Stabil. 89 (2005) 233.
[45] A. Habibi, J. De Wilde, Int. J. Chem. React. Eng. 5 (2007), art. A97.
[46] R. Steele, M. Jacobs, J. Appl. Polym. Sci. 2 (1959) 86.
[47] R.T. Conley, P.L. Valint, J. Appl. Polym. Sci. 9 (1965) 785.
[48] H.C. Beachell, S.P. Nemphos, J. Polym. Sci. 25 (1957) 173.
[49] R. Parthasarathy, K.J. Rao, C.N.R. Rao, Chem. Soc. Rev. 12 (4) (1983) 361.
[50] G.H. Fredrickson, Ann. Rev. Phys. Chem. 39 (1988) 149.
[51] Y. Scheyer, C. Levelut, J. Pelous, D. Durand, Phys. Rev. B 57 (18) (1998) 1122.
[52] G.V. Kozlov, Y.S. Lipatov, Polym. Sci. B 45 (3–4) (2003) 71.
[53] L.H. Sperling, J. Polym. Sci. Polym. Symp. 60 (1977) 175;
L.H. Sperling, Polym. Mater. Sci. Eng. 60 (1989) 477.
[54] R.E. Wetton, R.D.L. Marsh, J.G. Van-de-Velde, Thermochim. Acta 171 (1) (1991) 1.
[55] D.S. Jones, Int. J. Pharm. 179 (2) (1999) 167.
[56] V.V. Krongauz, A.D. Trifunac (Eds.), Processes in Photoactive Polymers, Chapmann & Hall, New York, Albany, Bonn, Boston, Cincinnati, Detroit, London, Madrid, Melbourne, Mexico City, Paris, San Francisco, Singapore, Tokyo, Toronto, Washington, 1995.
[57] K.D. Belfield, J.V. Crivello (Eds.), Potoinitiated Polymerization, vol. 847, ACS Symp. Ser., Washington, DC, 2003.
[58] V.V. Krongauz, M.G. Sullivan, S.C. Lapin, E.J. Murphy, U.S. Pat. No. 6,265,476 (2001).
[59] V.V. Krongauz, A.J. Tortorello, J. Appl. Polym. Sci. 57 (13) (1995) 1627.
[60] V.V. Krongauz, C.P. Chawla, RadTech Europe 99, Conference Proceedings, November 8–10, 1999, p. 435.
[61] (a) Sartomer Co. Inc., publications 5060, and 4014, July, 2005; publication 2347, August, 2003;
(b) G. Socrates, Infrared Characteristic Group Frequencies, John Wiley & Sons, Chichester, New York, Brisbane, Toronto, 1980.
[62] L.W. Hill, Prog. Org. Coat. 31 (1997) 235.
[63] K. Demirelli, M.F. Coskun, E. Kaya, Polym. Degrad. Stabil. 78 (2002) 333.
[64] S. Zulfiquar, M. Zulfiquar, T. Kausar, Polym. Degrad. Stabil. 17 (1987) 327;
S. Zulfiquar, M. Zulfiquar, T. Kausar, Polym. Degrad. Stabil. 30 (1990) 195.
[65] V.V. Krongauz, E.R. Schmelzer, R.M. Yohannan, Polymer 31 (6) (1990) 1130;
V.V. Krongauz, E.R. Schmelzer, R.M. Yohannan, Mol. Cryst. Liq. Cryst. 183 (1990) 495;
V.V. Krongauz, E.R. Schmelzer, R.M. Yohannan, Polymer 32 (9) (1991) 1654;
V.V. Krongauz, E.R. Schmelzer, R.M. Yohannan, Polymer 33 (9) (1992) 1893.
[66] V.V. Krongauz, C.C. Legere, Polymer 34 (17) (1993) 3614.
[67] V.V. Krongauz, C.P. Chawla, RadTech 2000, Conf. Proc., April 9–12, 2000, p. 261;
V.V. Krongauz, C.P. Chawla, RadTech Asia 2001, Conf. Proc., May 15–19, 2001, p. 168;
V.V. Krongauz, C.P. Chawla, Proc. of 222nd ACS Nat. Meet., August 26–30, 2001;
V.V. Krongauz, C.P. Chawla, RadTech Report Sept./Oct. 34 (2001) 16.;
V.V. Krongauz, C.P. Chawla, in: K.D. Belfield, J.V. Crivello (Eds.), Photoinitiated Polymerization, ACS Symp. Ser. 847, Washington, DC, 2003, pp. 165–175 (Chapter 14).
[68] S.L. Madorsky, S. Straus, J. Res. Nat. Bur. Stand. 50 (1953) 165.
[69] J. Fourie, W.J. McGill, South Afr. J. Chem. 32 (2) (1979) 63.
[70] S.S. Zislina, N.A. Senina, L.M. Terman, U.D. Semchikov, Vysokomol. Soed. B: Kratk. Soobsh 15 (6 Pt. 1) (1973) 459.
[71] V.Z. Pogorelko, N.A. Karetnikova, A.V. Ryabov, Visokomol. Soed. B: Kratk. Soobsh 15 (8) (1973) 625.
[72] P. Dole, J. Chauchard, J. Appl. Polym. Sci. 65 (1997) 2507.
[73] V.V. Korshak, G.M. Tseitlin, V.N. Ryzhov, Dokl. Acad. Nauk SSSR 293 (4) (1987) 903.
[74] E.T. Gevorkyan, L.V. Barkova, Vysokomol. Soed. Ser. B: Kratkie Soobsh 19 (10) (1997) 758.
[75] R. Steele, J. Harvey, J. Appl. Polym. Sci. 2 (4) (1959) 86.
[76] S.J. Yoo, G.V. Pace, B.K. Khoo, J. Lech, T.G. Hartman, Radtech Report May/June (2004) 60.
[77] (a) J. Unwin, Development and analysis methods to measure airborne acrylate in UV-cured motor vehicle repair coatings, Health Saf. Lab. 2007/2008;
(b) S.D. Hanton, Chem. Rev. 101 (2001) 527.
[78] J.O. Herschfelder, C.F. Curts, R.B. Bird, Molecular Theory of Gases and Liquids, John Wiley & Sons, Chichester, New York, Brisbane, Toronto, Singapore, 1954.
[79] (a) H. Eyring, J. Chem. Phys. 37 (1936) 283;
(b) S. Glasstone, K.J. Laidler, H. Eyring, The Theory of Rate Processes, McGraw Hill, Ney York, 1941.
[80] H. Eyring, T. Ree, Proc. Natl. Acad. Sci. U.S.A. 47 (1961) 526.
[81] R. Simha, R.F. Boyer, J. Chem. Phys. 37 (1962) 1003.
[82] S.M. Aharoni, J. Appl. Polym. Sci. 23 (1) (1979) 223.
[83] D.W. Van Krevelen, Properties of Polymers: Their Correlation with Chemical Structure; Their Numerical Estimation and Prediction From Additive Group Contribution, 3rd ed., Elsevier, Amsterdam, Oxford, New York, Tokyo, 1990.
[84] A.M. North, Pure Appl. Chem. 54 (2) (1982) 247.
[85] Kh.S. Bagdasar'yan, Theory of Free-Radical Polymerization, Israel Program for Scientific Translations, Jerusalem, 1968.
[86] L.E. Nielsen, J. Macromol, Sci.-Rev. Macromol. Chem. C3 (1) (1969) 69.
[87] A.T. DiBenedetto, J. Polym. Sci. Part B: Polym. Phys. 25 (9) (1987) 1949.
[88] A.V. Tobolsky, D. Katz, M. Takahashi, R. Schaffhauser, J. Polym. Sci. A2 (1964) 749.
[89] J. Bicerano, R.L. Sammler, C.J. Carriere, J.T. Seitz, J. Polym. Sci. Part B: Polym. Phys. 34 (1996) 2247.
[90] V.R. Gumen, F.R. Jones, D. Attwood, Polymer 42 (13) (2000) 5717.
[91] V. Barboiu, M.I. Avadanei, Polymer 49 (2008) 4687.
[92] J.A. Morrill, R.E. Jensen, P.H. Madison, C.F. Chabalowski, Army Res. Lab., Aberdeed Proving Ground, MD 21005-5066 Report ARL-TR-3137, Feb. (2004).
[93] Y.S. Lipatov, Uspekhi Khimii 47 (2) (1978) 332.
[94] V.A. Kargin, G.L. Slonimsky, Dokl. Akad. Nauk SSSR 62 (1949) 239;
V.A. Kargin, G.L. Slonimsky, Zurn. Fizic. Chimii 23 (1949) 563;
V.I. Irshak, Dokl. Akad. Nauk 380 (1) (2001) 31;
P.E. Rouse, J. Chem. Phys. 21 (1953) 1272.
[95] G. Wilemski, M. Fixman, J. Chem. Phys. 60 (1974) 866.
[96] Yu.Ya. Gotlib, N.K. Balabaev, A.A. Darinskii, I.M. Neelov, Macromolecules 13 (1980) 602.
[97] H.-X. Zhou, J. Chem. Phys. 118 (4) (2003) 2010.
[98] S. Jun, J. Bechhoefer, B.-Y. Ha, Europhys. Lett. 64 (3) (2003) 420.
[99] R.M. Ziff, E.D. McGrady, Macromolecules 19 (10) (1986) 2513.
[100] D.S. Argyropoulos, H.I. Bolker, Macromolecules 20 (11) (1987) 2915;
D.S. Argyropoulos, H.I. Bolker, Macromol. Chem. 189 (1988) 607;
D.S. Argyropoulos, H.I. Bolker, J. Wood Chem. Technol. 7 (4) (1987) 499.
[101] P. Martens, A.T. Metters, K.S. Anseth, C.N. Bowman, J. Phys. Chem. B 105 (22) (2001) 5131.
[102] X.Z. Qin, A. Liu, A.D. Trifunac, V.V. Krongauz, J. Phys. Chem. 95 (15) (1991) 5822;
X.Z. Qin, A. Liu, A.D. Trifunac, V.V. Krongauz, J. Phys. Chem. 96 (1) (1992) 207.